Digital Microfluidics Using PDMS Microchannels

by

CHOW Wing Yin, Winnie

A Thesis Submitted in Partial Fulfillment

of the Requirements for the Degree of

Master of Philosophy

In

Automation and Computer-Aided Engineering

July 2004

ABSTRACT

In recent years, with the rapid development of biomedical researches, more and more tools are needed to manipulate cells, DNA, and other biological samples. As the sizes of these creatures are in micron or even nano scale, Micro Electro Mechanical Systems (MEMS) are suitable for these applications. The objective of this dissertation is to design digital microchannels using PDMS polymer. Electrowetting-on-dielectric principle is used to manipulate the droplet. A PDMS dielectric layer is used as the contact surface with the water droplet. When an electric potential is applied to the electrode, the charges on the dielectric surface redistributes, leading a change to the surface tension of the dielectric layer. The contact angle of the water droplet changes, results in movement of the water droplet. The microchannel is fabricated by soft lithography, which is a simple and fast method to fabricate polymer microchannels. Experimental results showed that water droplet could be transported in the PDMS microchannel. However, there were still rooms for improvement for the speed . Different parameters such as channel gap distance and thickness of PDMS were modified to improve the performance. Thickness was found to be the main factor affecting the speed. This microchannel can transport liquid droplet without using other mechanical devices such as micropump and microvalve.

摘要

近年來隨著生物醫學迅速發展,對操縱細胞,DNA 和其他生物樣本的工具產生了大量需求。由於這些樣本的大小只有微米甚至是納米,所以微米機電系統(MEMS)非常適合於這些應用。這篇論文的目標是設計用 PDMS 聚合物造成的數碼微型管道。利用電濕化理論操縱在電介質面上的微滴。用一層 PDMS 電介質作爲與微水滴的接觸面。當電壓供應予電殛時,那些在電介質面上的電子便會重新分配,使電介質的表面張力改變。微水滴接觸角的改變令微水滴移動。微型管道是用軟性平印技術來製成。這是一種快和簡單的製造聚合物微型管道技術。實驗結果顯示微水滴能在 PDMS 微型管道內行走。可是,速度還有加快的空間。不同的參數如管道的高度和 PDMS 的厚度也曾被修改來改善效率。相信 PDMS 厚度是影響速度的主要因素。這條微型管道能運送液體微滴而無需其他機械裝置如微型泵和微型活門等輔助。

ACKNOWLEDGEMENTS

I would like to first express my sincere gratitude and appreciations to my advisor Professor W. J. Li for providing me this opportunity to work in the research area of MEMS and also for his patience and support at all levels. I would also like to thank my dissertation committee, Professor R. Du, Professor Y. M. Wang and Professor G. B. Lee for reading my dissertation and giving me constructive comments.

Thanks to all the CMNS members, especially Camen F., Thomas L., Hoyin C., Jennifer Z., Raymond L., Tak Sing W., and Tony T., for their suggestions and help on my project, Alan L., King L., and Johnny L., for their computer technical support. My appreciations to Dr. W. Y. Cheung for permitting the fabrication of my projects at the Semiconductor Microfabrication Lab of the Department of Electrical Engineering, Mr. A. Lee from the Department of Physics, for providing me the bonding test equipments and SEM and others who gave assistance to my experiments.

To my friends at ACE, thank you Crystal, Eric, Angie, Captain, Ben and my best friends in CMNS, Carmen, King, Alan, and Johnny, for sharing the joyful moments.

Finally, I would like to give my deepest gratitude to my parents and sister, for their long-life love and support, especially when I was in my hard time.

TABLE OF CONTENTS

LIST OF FIGURES

LIST OF TABLES

CHAPTER ONE

INTRODUCTION

In the past decades, Micro Electro Mechanical Systems (MEMS) are greatly developed. Different types of microsensors and microactuators were successfully built. As technology becomes advance, people are more and more interested in the microscopic world. They find out that the rules in the microscopic world are different from the macro world. For example, fluid flows in small devices differ from those in macroscopic machines.

1.1 Digital Microfluidics

Microfluidics handling of fluids in microscale has gained much attention last several years. Due to the recent success in biotechnologies, many microfluidic devices are applied to biomedical researches. As a few early MEMS researchers set out to develop microfluidic devices in late 1980's, they only miniaturized similar existing device. Typical fluidic devices in conventional scale such as pumps to drive fluids and valves and nozzles to regulate fluids movement were fabricated. Numerous methods were used to operate these devices, including electrostatic, piezoelectric, thermopneumatic, electromagnetic, bimetallic, and shape memory alloy actuation.

Since many biomedical researches focus on manipulating cells and DNA, instead of continuous fluid flow, droplet manipulation is investigated is this project. Besides, digital microfluidic devices can also be applied to chemical mixing and analysis. As the

fluid in the device is a drop, the volume of the fluid can be well controlled. This makes the analysis results more accurate.

In microscale, surface tension force becomes the dominant force. Electrowetting principle, which is developed based on the change of the surface tension with an applied potential, is used to manipulate droplets in microchannels. However, the liquid droplet needs to be an electrolyte. Also, when the voltage is applied to the droplet for a period of time, electrolysis occurs.

In order to solve this problem, a dielectric layer is inserted between the electrode and the liquid droplet. This phenomenon is called electrowetting-on-dielectric (EWOD). Droplet transporting, cutting, and merging can be performed in a microchannel by switching the electrodes between ground and activated states.

1.2 Soft Lithography of Polymer

In order to apply the device in biomedical field, biocompatible materials are used as the structural materials of the microchannel. Polymers are ideal materials for this microchannel. Besides the electrodes, all other materials of the microchannel are polymers. The advantages of using polymers are inexpensive, transparent, and many of them are biocompatible. PMMA is chosen to be the substrates. PDMS, which is an elastomer, is used as the structural materials and dielectric layers. Even the material of the mold structure for fabricating PDMS microchannel is also a polymer, SU-8.

Unlike the traditional fabrication process, the microchannel patterns on the PDMS are fabricated by replica molding technique. A mold master is fabricated first, and then the PDMS prepolymer mixture is spun on the mold and cured. This technique is simple

and fast. By using the special characteristic of PDMS, the fabricated microchannel is finally sealed by oxygen plasma.

This dissertation discusses the fabrication process of the microchannel and the experimental results of droplet transporting in the microchannel. Two common techniques that are used to control the surface tension: (i) thermocapillary-based microactuation and (ii) electrocapillary-based microactuation are presented in Chapter two.

The PDMS microchannels were fabricated by various processes. The soft lithography technique that was used to fabricate PDMS is presented in Chapter three. Metal electrodes were deposited by sputtering. However, the adhesion between the gold electrodes and PDMS layer was not good. Therefore, an additional adhesion layer was needed. Parylene C was chosen as the adhesion layer. The details are discussed in Chapter four.

Besides using PDMS as the structural material of the microchannel, PDMS can be used as a bonding interface to bond two PMMA substrates. The bonding technique is presented in Chapter five.

The electrowetting-on-dielectric principle that was used in the microchannel to manipulate the droplet is presented in Chapter six. In this chapter, the detailed design of the microchannel is also discussed. After the microchannels were fabricated, the samples were tested. Water droplet was successfully transported in the PDMS parallel plate microchannel. However, the speed could still be improved. Several parameters were modified to improve the performance. The details are discussed in Chapter seven. A digital microfluidic circuit was proposed as a further development of the project. The

design is presented in Chapter eight. Finally, a summary of this dissertation is provided in Chapter nine.

CHAPTER TWO

ELECTROCAPILLARY-BASED MICROACTUATION

When the size of creatures is decreased to submillimeter scale, surface tension becomes the dominant and effective force. Therefore, liquid handling and actuation by controlling surface tension has many advantages in microscale applications. Electrowetting-on-dielectric (EWOD) applies to aqueous liquid by varying electric energy across the thin dielectric film between the liquid and conducting substrate. By electrically changing the wettability of the electrode, a liquid on these electrodes can be shaped and driven along the active electrodes, making microfluidics extremely simple for both device fabrication and operation. By using EWOD, the mechanism becomes more effective as the size of the device becomes smaller.

2.1 Surface Tension in Microscale

Surface tension is a unique type of force, which scales directly to length. It becomes dominant over pressure (surface force) or mass (body force), when the dimension of interest shrinks down to sub-millimeter range. In the MEMS world, surface tension is closely related to stiction problem, which has been one of the main problems. However, in recent years, researches have been focused on utilizing surface tension in other areas. Surface tension is used to stabilize small objects, such as applying to inkjet printers for preventing ink from leakage. In the microfluidics field, it is used to induce motion for liquids. Many methods were developed to control the surface tension, such as chemical

(i.e., use of surfactant), thermal (i.e., thermocapillary), and electrical methods (i.e., electrocapillary).

2.2 Thermocapillary-Based Microactuation

Thermocapillary-based microactuation uses microfabricated heaters to create a temperature gradient in a column of liquid or bubble, generating a surface tension gradient that causes liquid to flow. An example is a valveness micropumping of liquid [1]. The microdevice in Figure 2.1 was originally designed to pump fluid in a microchannel using thermocapillary effect. With proper current pulses to the heaters, the initially created bubble simply grows at one end (right side in the figure) and shrinks at the other end (left side in the figure). As the surface tension is higher at one end than the other due to the temperature gradient existing along the channel, the bubble applies a pressure to the liquid in the microchannel.

The thermal driving mechanism, however, suffers from such limitations as high power consumption, heating of liquid, quick evaporation, and slow speed (governed by cooling).

2.3 Electrocapillary-Based Microactuation

Electrocapillary-based microactuation, which is different from thermocapillary-based microactuation, involves no heating of the liquid. Electrocapillary principles are all based on the fact that surface tension is a function of electric potential across an interface. Depending on the types of interfaces and phases involved, they can be classified into three principles: continuous electrowetting (CEW), electrowetting

(EW), and electrowetting-on-dielectric (EWOD). Compared with thermocapillary-based microactuation, electrocapillary-based microactuation is much more energy efficient and advantageous for most microfluid actuations.

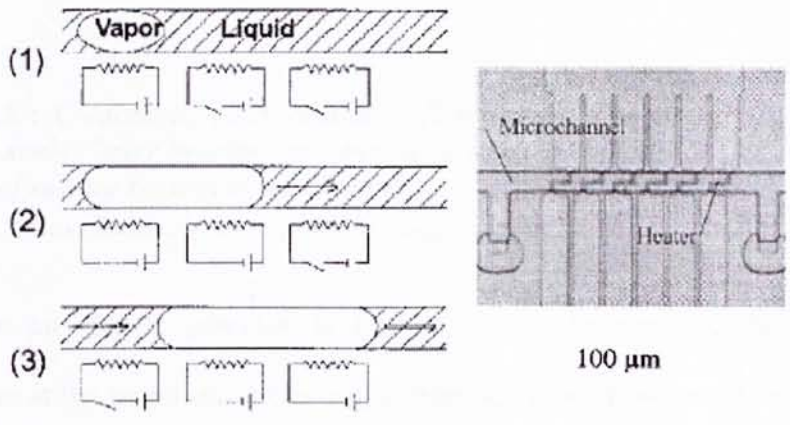

Figure 2.1 : *Valveless micropump using bubbles. Left: the bubble moves under thermal gradient, pumping the liquid along the channel. Right: picture of fabricated device. (Reprint from [1].)*

2.3.1 Continuous Electrowetting (CEW)

Continuous electrowetting (CEW) refers to a principle of moving a lump of liquid metal in a liquid medium using electric potential. For example, as shown in Figure 2.2, a liquid metal droplet (e.g., mercury) travels along an electrolyte-filled channel or tube when an electric potential is applied across the length of the channel. The movement of a mercury slug in electrolyte is due to the local change of surface tension.

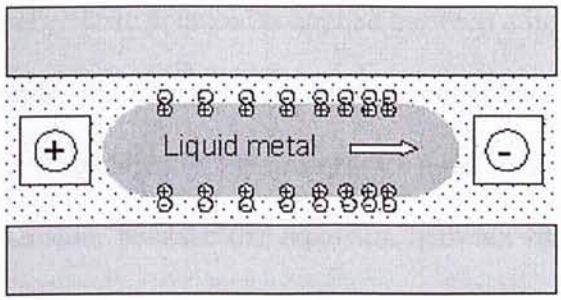

Figure 2.2 : *Continuous electrowetting (CEW) effect. The charge distribution at electrical double layer becomes asymmetrical, when the voltage is applied, inducing variation of surface tension along channel.*

When an electric potential is applied across the channel, the electric charge distribution at the liquid metal-electrolyte interface is as shown in Figure 2.2. A surface tension gradient is produced according to the Lippman's equation [2], and motion is induced. The electric potential across the electrical double layer (EDL) becomes higher near the negative electrode. The surface tension decreases as the potential drop (across EDL) increases and the motion occurs to the right where the surface tension is lower. Movement of the droplet to the lower surface-tension area can also be interpreted as the tendency to minimize the energy by wetting the low surface tension region more than the higher one. CEW effect has been realized with MEMS applications [3] [4] [5].

2.3.2 Electrowetting (EW)

Compared with CEW, electrowetting (EW) does not need to be operated in electrolyte medium, instead, it can be operated in air medium. It can manipulate any electrolyte droplets other than only liquid metal droplet. The operating principle is

shown in Figure 2.3.

When an external electric potential is applied between a liquid and solid or between two immiscible liquids, the charges and dipoles redistribute, modifying the surface energy at the interface. Specifically, the presence of a net electric charge at an interface lowers the surface tension, because the repulsion between like charges decreases the work done in expanding the surface area. The mathematical relationship between the applied electric potential (V) and the resulting surface tension (γ) can be derived by thermodynamic analysis of the interface. The result is expressed in Lippmann's equation [2]:

$$\gamma = \gamma_0 - \frac{1}{2} C V^2 \qquad \text{Eq. 2.1}$$

where γ_0 is the surface tension of the solid-liquid interface at the potential zero charge (i.e., no charge at the surface of the solid), and C is the capacitance per unit area, assuming the charge layer can be modeled as a Helmholtz capacitor. In Figure 2.3, C in Eq. 2.1 corresponds to the capacitance of the electric double layer (EDL) formed at metal-electrolyte interface.

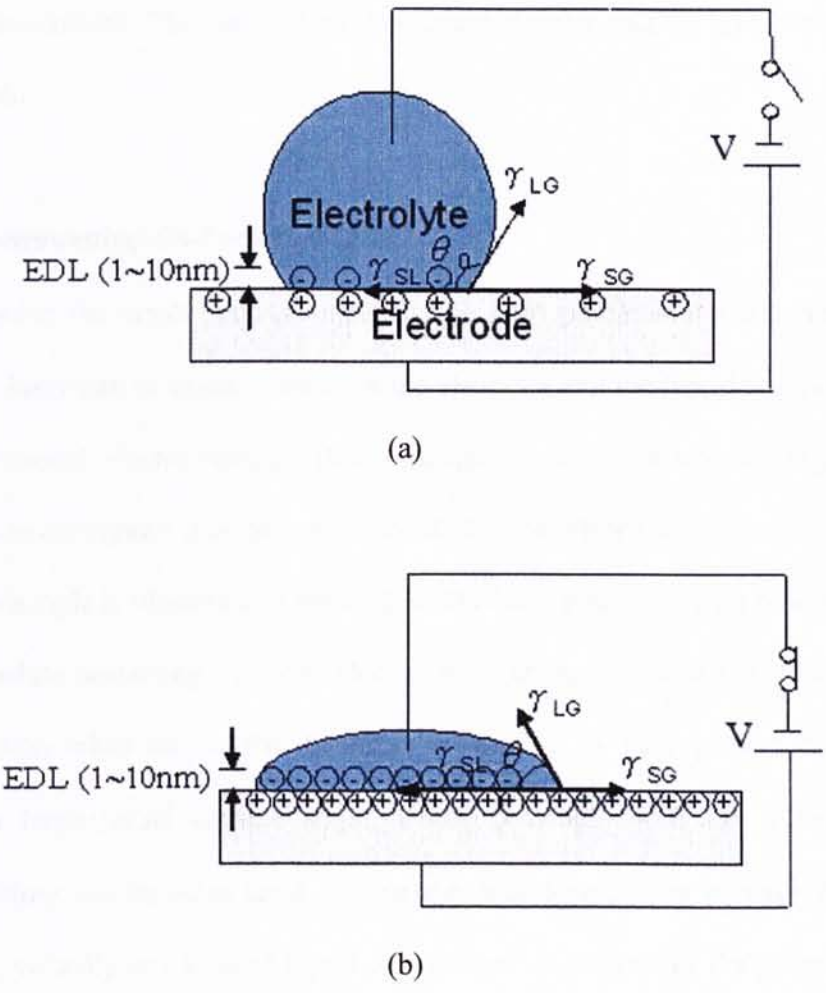

Figure 2.3 : *Principle of electrowetting. (a) No external voltage applied. Charges are distributed at the electrode-electrolyte interface, building an EDL. (b) External voltage applied. Charge density at EDL changes so that γ_{SL} and the contact angle decrease or increase.*

However, this electrowetting is only useful with combinations of metal electrode and electrolytes that can generate a polarizable interface. Since only a small voltage drop can be sustained across the EDL, the contact angle change ($\Delta\theta$) that can be induced by conventional electrowetting is relatively small, limited by electron transfer from the

electrode to redox-active species in the liquid. Furthermore, gas bubbles are produced due to electrolysis. This may block the liquid droplet motion and make the motion irreversible.

2.3.3 Electrowetting-On-Dielectric (EWOD)

To solve the small contact angle change ($\Delta\theta$) problem of electrowetting, a thin dielectric layer can be inserted between the electrode and the liquid to emulate the EDL in conventional electrowetting. This principle is called electrowetting-on-dielectric (EWOD) to distinguish it from conventional electrowetting on conductive surfaces. The EWOD principle is illustrated in Figure 2.4. The ideal dielectric layer blocks the electron transfer, while sustaining the high electric field at the interface that results in charge redistribution when an electric potential is applied. A hydrophobic dielectric layer creates a large initial contact angle, which provides room for a large $\Delta\theta$ upon electrowetting. On the other hand, by inserting a dielectric layer between the liquid and electrode, virtually any kind of liquid can be used, regardless of the polarization of the interface.

Lippmann's Eq. 2.1 can be expressed in terms of the contact angle θ by incorporating Young's Eq. 2.2. The resulting equation (Eq. 2.3) is called the Lippmann-Young equation.

$$\gamma_{SL} = \gamma_{SG} - \gamma_{LG}\cos\theta \qquad \text{Eq. 2.2}$$

$$\cos\theta = \cos\theta_0 + \frac{1}{\gamma_{LG}}\frac{1}{2}CV^2 \qquad \text{Eq. 2.3}$$

In Eq. 2.3, θ_0 is the contact angle when the electric field across interfacial layer is zero, γ_{SL} is the solid-liquid surface tension, γ_{LG} is the liquid-gas surface tension, and γ_{SG} is the solid-gas surface tension. Note that γ_{LG} and γ_{SG} are assumed to be constant, independent of the applied potential.

The contact angle in Eq. 2.3 is a function of the applied voltage between the liquid and electrode. Eq. 2.3 also implies that using a high capacitance dielectric layer would lower the voltage required to obtain a given $\Delta\theta$. The specific capacitance of a dielectric layer is

$$C = \frac{\varepsilon_0 \varepsilon}{t} \qquad \text{Eq. 2.4}$$

where ε_0 is vacuum permittivity, ε is the dielectric constant of the dielectric material, and t is the thickness of the dielectric layer.

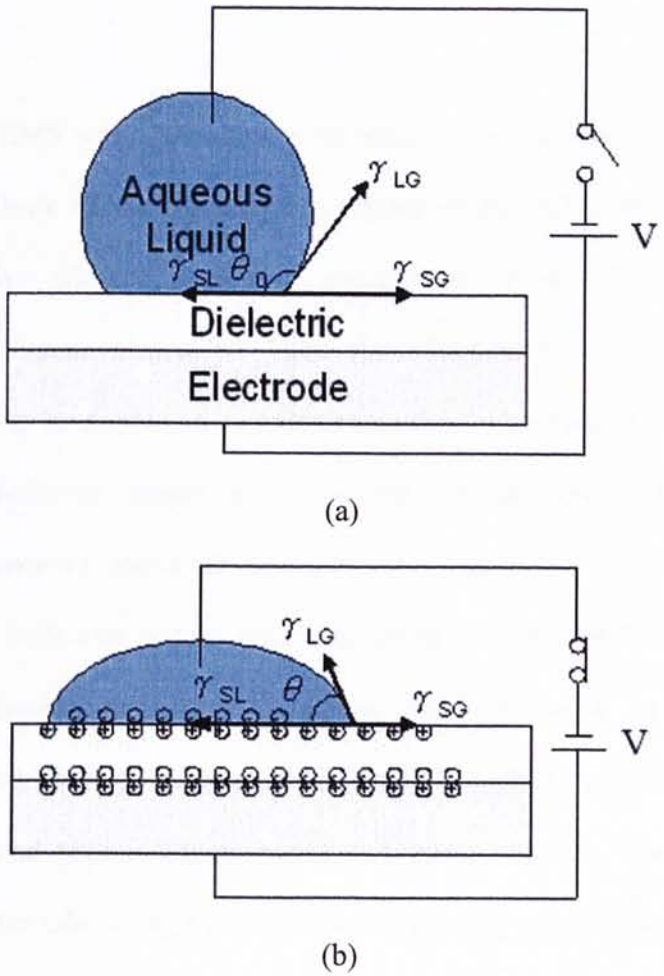

Figure 2.4 : *Principle of EWOD. (a) With no external voltage applied, there is no charge accumulation at the interface. (b) With an external voltage applied, charge accumulates at the interface.* γ_{SL} *and the contact angle* θ *decrease.*

CHAPTER THREE

SOFT LITHOGRAPHY

In the MEMS world, the most widespread fabrication methods to produce MEMS structures are bulk micromachining and surface micromachining. Bulk micromachining is a subtractive fabrication method where single-crystal silicon is lithographically patterned and then etched to form three-dimensional (3D) structures. Surface micromachining, in contrast, is an additive method where layers of semiconductor-type materials (polysilicon, metals, silicon nitride, silicon dioxide, etc.) are sequentially added and patterned to make 3D structures.

However, bulk and surface micromachining methods are limited by the materials used. The semiconductor-type materials typically used in bulk and surface micromachining are stiff materials with Young's modulus ~100GPa [6]. Furthermore, etching in Si and glass is too expensive and time-consuming. Therefore, new methods and materials for fabricating MEMS devices especially microfluidic systems are needed. Polymer, in contrast to silicon and glass, is inexpensive; channel can be formed by molding or embossing rather than etching. An alternative fabrication technique based on replication molding is becoming popular. Soft lithography is a fabrication technique, which an elastomer is patterned by curing on a micromachined mold. Its advantages include the capacity for rapid prototyping, easy fabrication without expansive capital equipment, and forgiving process parameters. In this chapter, PDMS microchannels fabricated by soft lithography method are introduced.

3.1 Rapid Prototyping

The rapid prototyping began with creating a design in a computer software program (Tanner EDA L-edit Pro). Then, the design was printed on a transparency by the high-resolution commercial laser printer system. The transparency film was used as mask in contact photolithography to generate master with a negative-tone UV photoresist (MicroChem Corporation Nano™ SU-8 2075, Newton, MA) on PMMA substrates. The detailed process for making the SU-8 master is in Appendix AII. This master was used for casting the PDMS channels. Figure 3.1 shows the process flow for rapid prototyping and Figure 3.2 is the photo of the SU-8 mold.

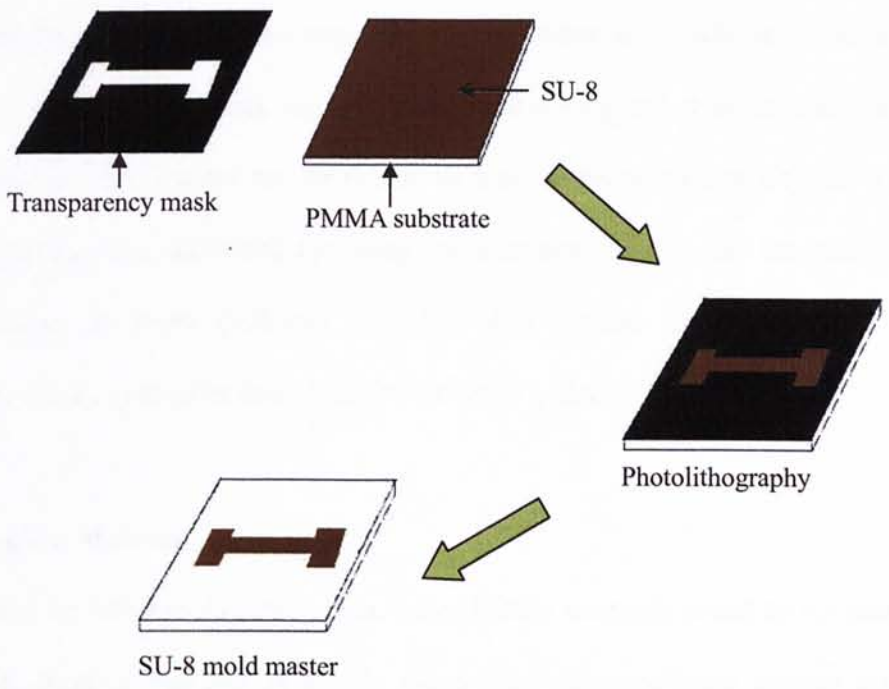

Figure 3.1 : *Scheme for rapid prototyping and replica molding of microchannel in PDMS.*

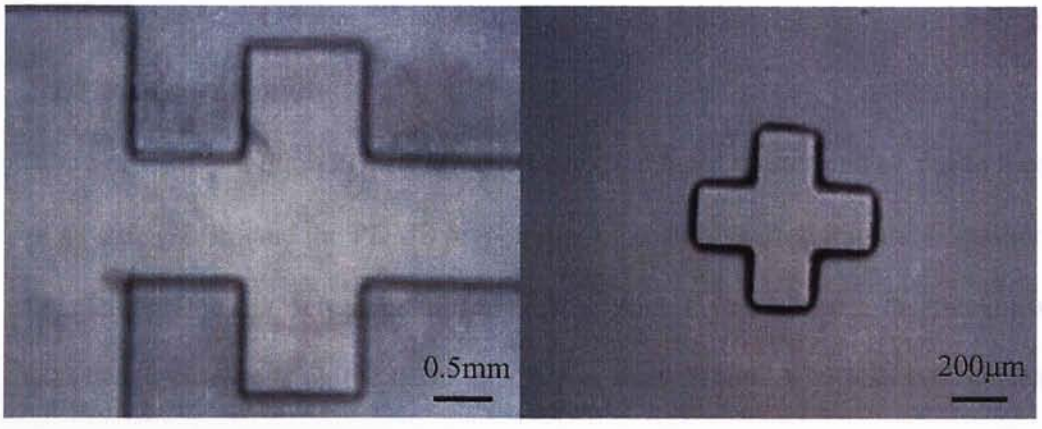

Figure 3.2 : *Photos of SU-8 mold.*

The advantage of rapid prototyping is the reduction in time and cost for a cycle of design, fabrication, and testing of new ideas compared with methods that use a chrome mask in the photolithography step. The chrome mask is 20-100 times more expensive than the transparency mask used in rapid prototyping and it takes hours to make. In addition, the mold master can be reused so that the fabrication process is very fast and cost effective. The drawback for using transparency mask is that the resolution of the transparency is lower (>20μm) than that of a chrome mask (~500nm). Therefore, features those are smaller than 20μm still require a chrome mask to make.

3.2 Replica Molding

After the SU-8 mold master was made, PDMS channels could be formed by replica molding. Replica molding is simply the casting of prepolymer against a master and generating a negative replica of the master in PDMS, i.e., ridges on the master appear as valleys in the replica. There are different methods for making both thick and thin PDMS

layers.

3.2.1 Pouring Method

For casting a thick PDMS layer (>1mm), the mold master can be put in a container (e.g., a petri dish) and the PDMS prepolymer mixture is poured into the container to cure [7]. This method is only suitable for making thick layers because the thickness of the PDMS layer depends on the depth of the container. Figure 3.3 illustrates the scheme of this method.

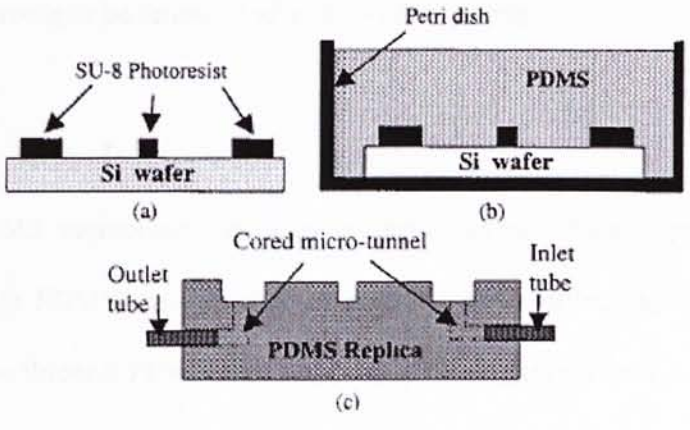

Figure 3.3 : *Scheme for fabricating a thick layer of PDMS using a petri dish. (Reprint from [7].)*

3.2.2 Sandwich Molding Method

Thin PDMS membrane (<1mm) can be fabricated by the sandwich molding method [7]. Figure 3.4 illustrates schematically the sandwich molding procedure. After the PDMS prepolymer mixture was poured onto the master, a transparency film was placed over the prepolymer mixture. The transparency film was carefully lowered onto the

prepolymer mixture, allowing surface tension to pull the transparency into intimate and continuous contact with the prepolymer mixture to prevent any bubbles formed at the interface. The flexible transparency film provided an easy way to remove the cover plates from PDMS molds after curing. The master-prepolymer-transparency stack was clamped within a sandwich that includes flat aluminum plates (top, bottom), a rigid Pyrex wafer, and a rubber sheet (~4mm thick). The clamped PDMS prepolymer sandwich was cured for 3 hours at 65°C on a hotplate. After curing, the thin PDMS replicas were peeled off from the masters. The thickness of the thin PDMS could be controlled by adding different weights to the clamp. One disadvantage of this method is that there is excess PDMS squeezed out from the master and cumulates at the edge of the master. It needs to be removed after every fabrication.

3.2.3 Spin-On Method

Thin PDMS membrane can also be made by traditional spin-on method. The spinning rate of PDMS (mixing ratio of prepolymer to curing agent 10:1) is shown in Figure 3.5. The thinnest PDMS that can be made with this method is ~5μm. The spin-on PDMS was cured on a 65°C hotplate for 3 hours. The cured PDMS membrane was then peeled off from the master. The thickness of the PDMS membrane can be well controlled by the spinning rate of the spin coater. There is one limitation of this method. The thickest PDMS membrane that can be made is ~100μm with the slowest speed of the spin coater (~500rpm). This method is suitable for making PDMS membrane with thickness between 5μm and 100μm.

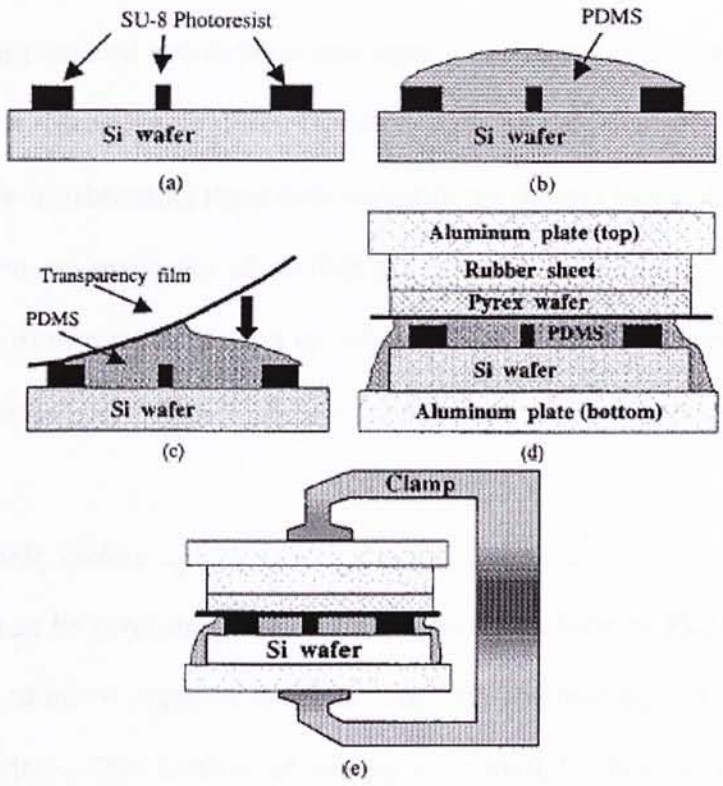

Figure 3.4 : *Schematic illustration of the sandwich molding process for thin layer of PDMS. (Reprint from [7])*

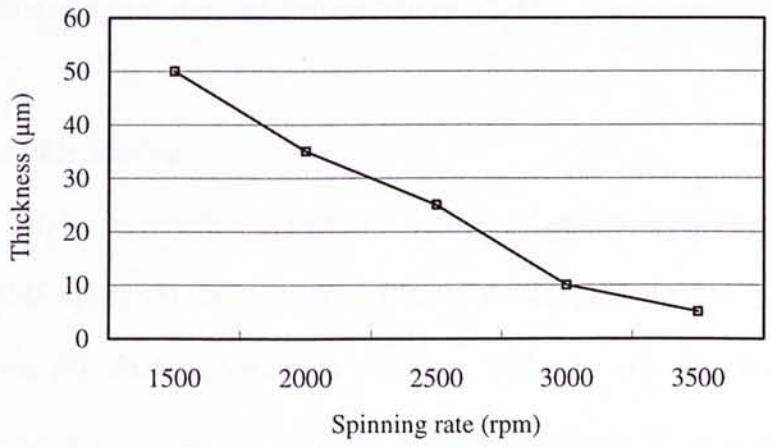

Figure 3.5 : *Thickness of spin-coated PDMS versus spinning rate.*

3.3 Sealing

After the patterned two-dimensional layer is fabricated from replica molding, one more layer is necessary to form the three-dimensional channel. Sealing plays an important role in fabricating these three-dimensional devices especially for microfluidic devices. There are two types of sealing: (i) reversible, conformal sealing with a flat surface, and (ii) irreversible sealing to certain substrates upon exposure of both surfaces to oxygen plasma.

3.3.1 Reversible Sealing

PDMS can be reversibly sealed to other materials because PDMS is flexible and can conform to minor imperfections in a "flat" surface making van der Waals contact with this surface. This method of sealing is watertight, fast, and occurs at room temperature. This reversible seal can be broken by peeling the PDMS off the surface. Removal of the PDMS leaves little or no residue on the other material, and resealing can occur numerous times without degradation in the PDMS.

3.3.2 Irreversible Sealing

PDMS can be irreversibly sealed to a number of materials by exposing to oxygen plasma: PDMS, glass, Si, SiO_2, quartz, silicon nitride, polyethylene, polystyrene, and glassy carbon [8]. PDMS comprises repeating unit of $-O-Si(CH_3)_2-$. Exposing PDMS to oxygen plasma introduces polar groups on the surface. The plasma introduces silanol groups (Si-OH) at the expense of methyl groups ($Si-CH_3$) [9] [10]. The silanol groups then condense with appropriate groups (OH, COOH, ketone) on another surface

when the two layers are brought into conformal contact. For PDMS and glass, this reaction yields Si-O-Si bonds after loss of a water. These covalent bonds form the basis of a tight, irreversible seal: attempting to break the seal results in failure in the bulk PDMS [8]. This method, however, does not work with all polymers, e.g., Saran, polyimide, poly(methylmethacrylate), and polycarbonate [8]. We can see that PDMS is a good sealing material. We have used it to be the bonding interface of polymer substrates and obtained satisfactory results. Details will be discussed in Chapter five.

3.4 Multilayer Fabrication

The irreversible sealing of PDMS to PDMS enables the fabrication of multilayer devices [6] [7]. This is very important to microfluidics. The ease of producing multilayer makes it possible to have multiple layers of fluidics, which is a difficult task with conventional micromachining. Because the devices are monolithic (i.e., all of the layers are composed of the same material), interlayer adhesion failures and thermal stress problems are completely avoided. This process can be used to construct complex multilayer microfabricated structures such as optical trains and microfluidic valves and pumps for lab-on-a-chip applications.

CHAPTER FOUR

METAL DEPOSITION

A layer of conductive electrode has to be deposited on each bottom and top layer of the microchannel to apply a potential. Gold (Au) electrodes are often used because of its good conductive property. Indium-tin-oxide (ITO) is also used as the electrode material because it is transparent [11]. It is good for observation. A good adhesion between metals and other structural materials is crucial for the device to function well. Sputtering methods were mainly used to deposit metals. The deposition of metals on different polymers is discussed in this chapter.

4.1 Gold Deposition by Sputtering Method

4.1.1 Gold Deposition on PMMA

A thin layer (~2500Å) of gold (Au) was deposited on PMMA substrate. However, it was found that the adhesion between Au and PMMA substrate was not good. The Au came off when the substrate was washed with acetone during the photolithography process. Several metals such as chromium (Cr), nickel (Ni), and titanium (Ti) were used as the adhesion layer between the PMMA substrate and Au layer, but the results were not satisfactory. Besides metals, parylene C was also used as the adhesion layer and satisfactory results were obtained. The process flow is shown in Figure 4.1.

4.1.2 Gold Deposition on PDMS

Due to the softness of PDMS, PDMS was first cured on a PMMA substrate before the Au deposition. However, the Au cracked after deposit on the PDMS as shown in Figure 4.2. The crack sizes were ~8μm wide. Attempts were made to eliminate these cracks by varying parameters such as Au film thickness and deposition temperature. It was found that no crack appeared again when the substrate temperature was increased to 100°C. The substrate was only heated to 100°C because the glass transition temperature (T_g) of the PMMA substrate is 105°C. Temperature higher than T_g would melt the substrate.

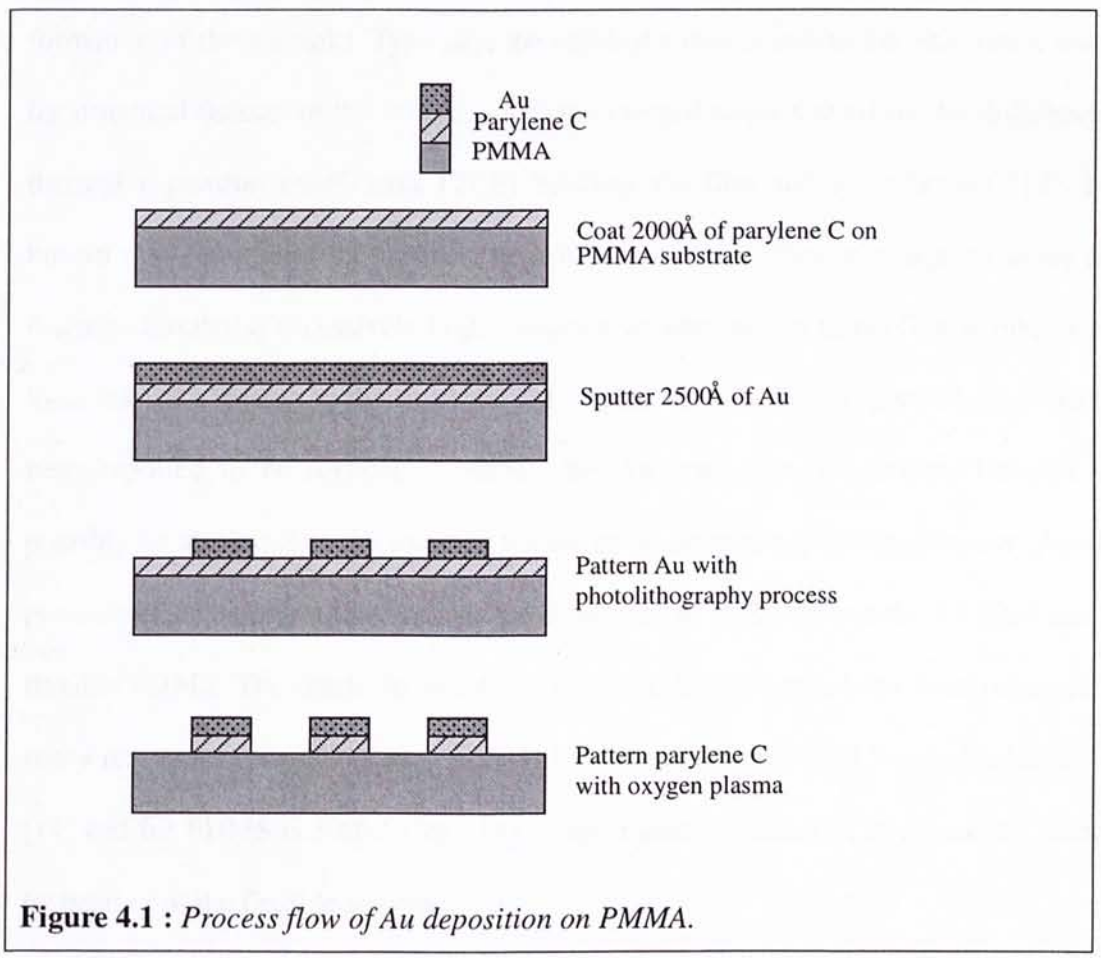

Figure 4.1 : *Process flow of Au deposition on PMMA.*

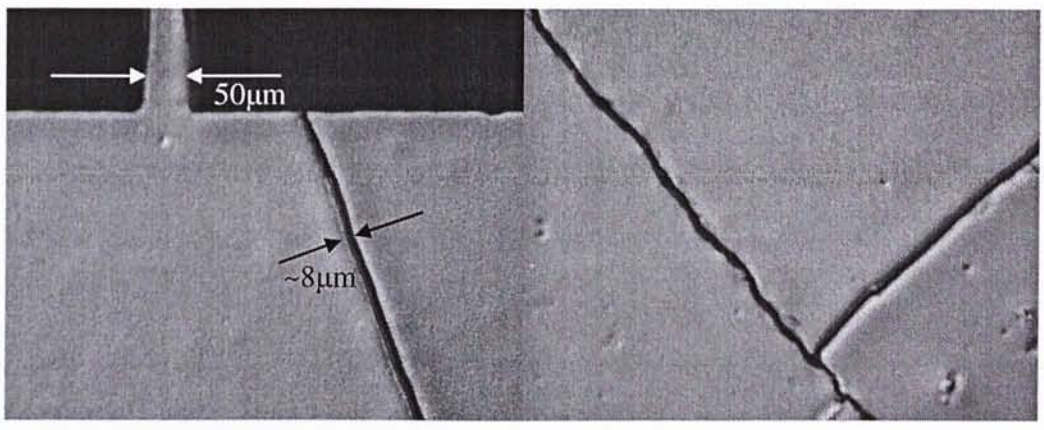

Figure 4.2 : *Samples of cracked metal films on the PDMS.*

The residual stress present in the deposited thin Au film is a possible cause for the formation of these cracks. Typically, the residual stress is due to intrinsic stress caused by structural defects in the thin film and the thermal stress caused by the difference in thermal expansion coefficients (TCE) between the film and the substrate [12]. It is known that sometimes the intrinsic tensile stresses are sufficiently large to cause film fracture. Similarly, excessively high compressive stresses can cause film wrinkling and local loss of adhesion to the substrate [12]. Since the stress of evaporated Au films has been reported to be invariantly tensile, the Au cracks on the flexible material can possibly be attributed to the intrinsic tensile stress from the sputtering process. Another possible explanation for the cracks is the difference in TCE between the Au films and the flexible PDMS. The cracks in thin films due to TCE mismatch have been observed by many researchers (i.e., Jorgensen et al. [13]). Since the linear TCE for Au is14.2×10^{-6}/K [14] and for PDMS is 590×10^{-6}/K [15], a significant mismatch in strain can be induced by heating of the flexible substrates.

The elimination of these cracks is important as they will limit the minimize size of patternable structures with good edge definitions. Experiments showed that the difference in TCE can be minimized by increasing the PDMS substrate temperature during the sputtering process. Samples of metal structures with no cracks on a flexible PDMS are shown in Figure 4.3 below.

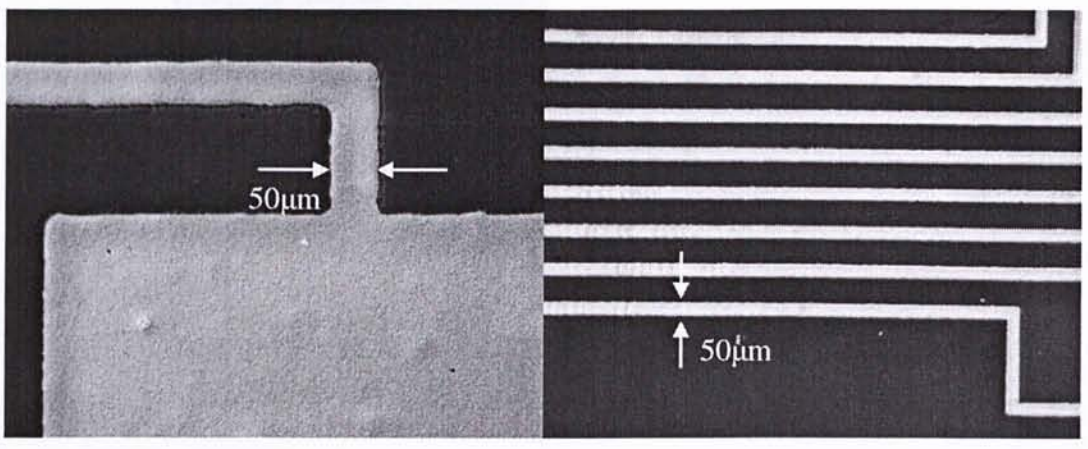

Figure 4.3 : *Crackless metal film structures on PDMS.*

Apart from the residual stress problem, the adhesion between PDMS and Au was not good. The Au film came off after dipping the structure in acetone for photoresist removal. From the experience of PMMA substrate, parylene C was used to be the adhesion layer between PDMS and Au film. Satisfactory results were obtained. The parylene C adhesion layer also solved the residual stress problem. No crack existed and no heating was required during the sputtering process. The process flow of Au deposition on PDMS is shown in Figure 4.4.

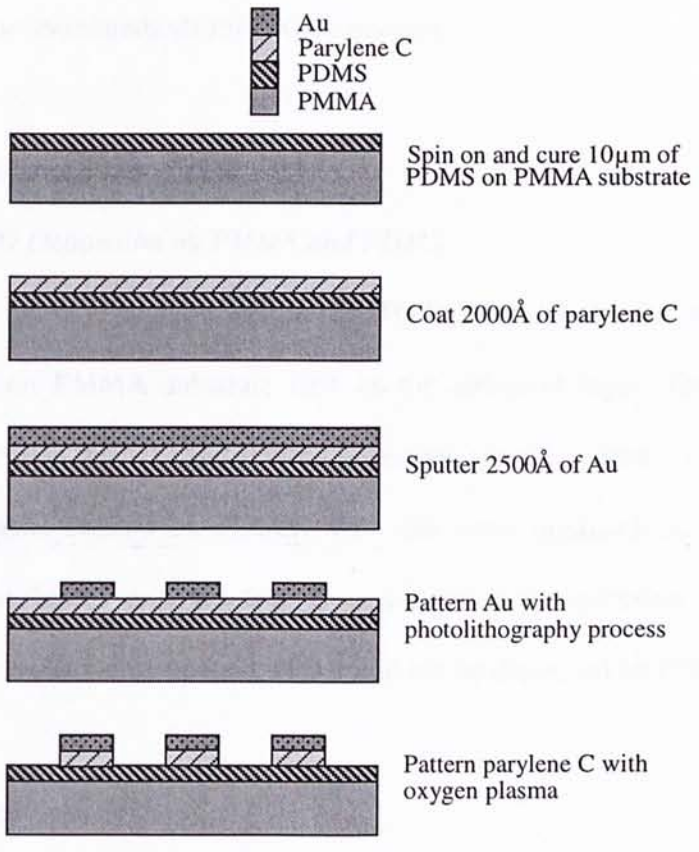

Figure 4.4 : *Pattern flow of Au deposition on PDMS.*

4.2 ITO Deposition by Sputtering Method

In recent years, various methods of preparation have been tried [15] for developing transparent conducting oxide films owing to their many practical applications. Usually, doped indium oxide and tin oxide films are used for this purpose because of their high transparency and conductivity. These oxide films are used in solar cells to serve simultaneously as conducting electrode and antireflection coating. Indium tin oxide (ITO) structure solar cells have been fabricated [16] in which the ITO layer serves as a transparent window and antireflection coating. These films are also used as selective

filters for solar thermal collectors and in liquid crystal displays. Reactive sputtering is one of the common methods for ITO deposition.

4.2.1 Image Patterning of ITO

4.2.1.1. ITO Deposition on PMMA and PDMS

Similar to Au deposition, before the ITO layer was deposited, a layer of parylene C was coated on PMMA substrate first as the adhesion layer. This can enhance the adhesion between the ITO and PMMA substrate. On the contrary, due to residual stress problem, cracks existed on PDMS. With the same approach of Au deposition, the substrate was heated and parylene C was used as the adhesion layer. However, no satisfactory results were obtained. ITO could not be deposited on PDMS.

4.2.1.2. Etching of ITO

One of the problems in using ITO with standard device processing is the necessity of well-controlled etching to define device electrodes down to micron level. The commonly used wet chemical etching technique with HCl based solutions for ITO produces etching underneath the photoresist mask. This poor control over pattern makes fabrication of near micron structures very difficult. Moreover, the HCl based etching solution attacks the PMMA substrate of our device. Therefore, wet etching is not suitable in our case.

Dry etching using a metal mask was proposed [17]. The argon (Ar) dry etching was found to obtain a satisfactory result. The etching rate of ITO using Ar plasma is shown in Figure 4.5. The method was followed. A 3000Å ITO layer was deposited on a PMMA

substrate by DC sputtering. The sample was then patterned using standard photolithography to enable thickness measurements following dry etching. According to Figure 4.5, the etching time should be around 90-100mins. However, after the sample was etched over 100mins, the ITO still could not be etched.

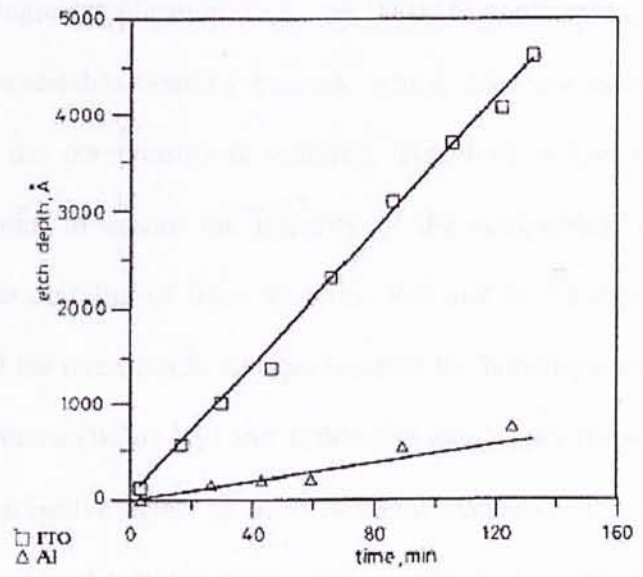

Figure 4.5 : *Etching depth against time using pure Ar plasma at 100W of power. (Reprint from [16].)*

CHAPTER FIVE

POLYMER-BASED SUBSTRATES BONDING USING PDMS

In recent years, polymer-based microfluidic devices have become increasingly important in biological applications (e.g., see [18]). To implement a microfluidic system, a reliable and repeatable bonding process, which does not alter the properties and performance of the components is required. Therefore, a low temperature bonding process is essential to ensure the integrity of the components during the bonding, packaging and assembling of these systems. Polymer is the most common adhesive bonding material for microfluidic devices because the bonding temperature is relatively low. Benzocylobutene (BCB) [19] and Teflon-like amphorous fluorocarbon polymer [20] are used as the adhesive layers to bond different materials such as silicon and glass. However, their required bonding temperature is still over 100°C. For glass and silicon substrates bonding, bonding over 100°C is still acceptable; but for polymer substrates bonding, this would greatly affect the bonding performance. A newly developed low temperature bonding technique using PDMS as the interface will be presented in this chapter. A microfluidic system consists of a micropump and microchannel was successfully fabricated.

5.1 Design of Microfluidic System

5.1.1 PDMS

PDMS, an elastomeric polymer, which is biocompatible, transparent, permeable to

gases and low cost, is becoming more popular among the microfluidic device community. Replica molding technique is commonly used to fabricate PDMS microfluidic devices [21]. The preparation process of PDMS is also simple. In addition, its low curing temperature (<100°C) makes it an excellent material for bonding polymer substrates since many polymer substrates cannot withstand a high bonding temperature (>200°C). Currently, PDMS is widely used as the structural material for microfluidic devices because of its biocompatibility and low cost properties. 3-D microchannels can be made easily and rapidly by replica molding method. Typically 3-D channels are formed by exposing both PDMS layers to oxygen plasma and then bonding them immediately after the plasma treatment [22]. PDMS can be irreversibly adhered to a number of materials such as glass, silicon and quartz [7]. However, PDMS cannot be adhered to PMMA by this method. Instead of using the oxygen plasma treatment, spin-coated PDMS was used as the interface to bond two PMMA substrates during the curing of PDMS.

5.1.2 Design of the Vortex Micropump

The vortex micropump uses the kinetic energy of an impeller and a circular pump chamber to move fluid [23]. The micro impeller is placed inside the pump chamber. When the fluid enters the micropump from the center of the impeller, the rotational motion of the impeller, driven by a DC motor, can induce fluid pressure with continuous flow. The vortex micropump was fabricated by the micro molding replication technique.

5.2 Fabrication of Microfluidic System

5.2.1 Micro Impeller Fabrication Process

The rotating impeller can induce pressure and generate the fluid flow. The fabrication process is shown in Figure 5.1. A layer of 200μm thick SU-8 negative photoresist was spun on a nickel substrate and was exposed under UV light with the mask of impeller pattern. After the SU-8 was developed, a 100μm thick nickel layer was electroplated on the substrate. The micro impeller was fabricated after removing the nickel and SU-8 substrate. The pattern and fringe profile is illustrated in Figure 5.2.

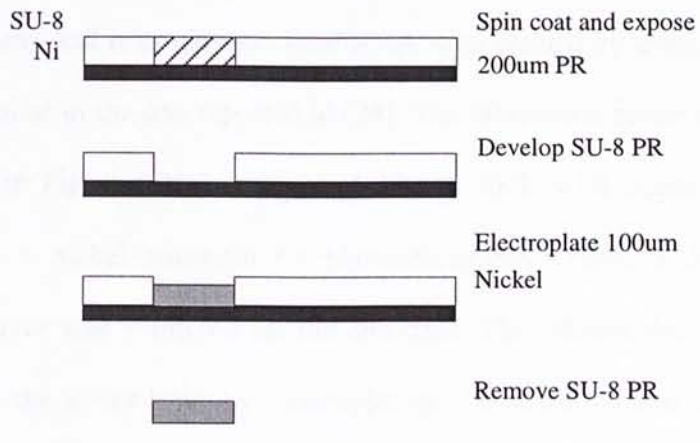

Figure 5.1 : *Fabrication of nickel micro impeller.*

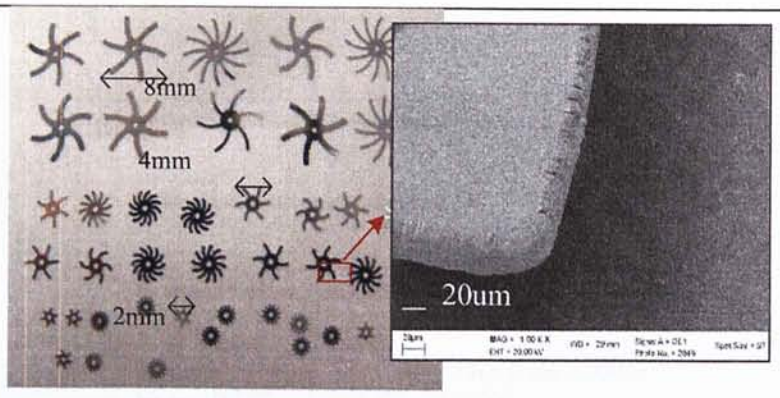

Figure 5.2 : *(Left) Photograph of nickel micro impellers and (Right) SEM image of one fringe of the impeller.*

5.2.2 Micro Patterning of PMMA by Hot Embossing Technique

Micropump and microchannel on PMMA were created by using the hot embossing technique similar to the one reported in [24]. The fabrication process used in our group is illustrated in Figure 5.3(a). A layer of 200μm thick SU-8 negative photoresist was patterned on a nickel substrate by photolithography. Then, a 3000Å thick silver conductive layer was sputtered on the substrate. The 300μm thick nickel mold was fabricated on the silver layer by electroplating. The mold pattern is shown in Figure 5.3(b). Nickel was used as the material of the metal mold because it is much harder than PMMA (Young modulus = 200GPa). The metal mold was then released and inserted into the hot embossing machine. The hot embossing machine used in our lab and its components are shown in Figure 5.4. The PMMA substrate was first heated to 120°C, which was slightly above the glass transition temperature of PMMA (T_g = 105°C). Then a pressure of 7MPa was applied by a hydraulic press to compress the mold towards the PMMA substrate, which allowed the channel pattern on the metal mold to be transferred to the PMMA substrate. The substrate and the mold were then cooled and separated.

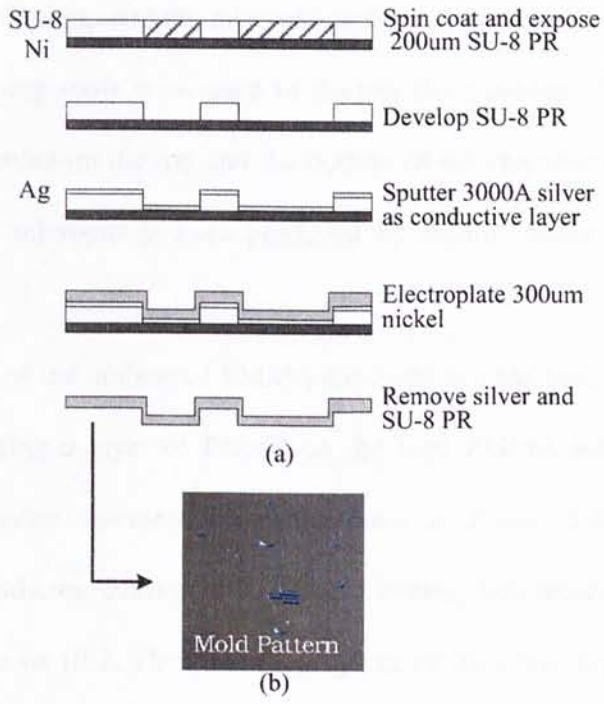

Figure 5.3 : *(a) Nickel micro mold fabrication process and (b) photograph of nickel micro mold pattern.*

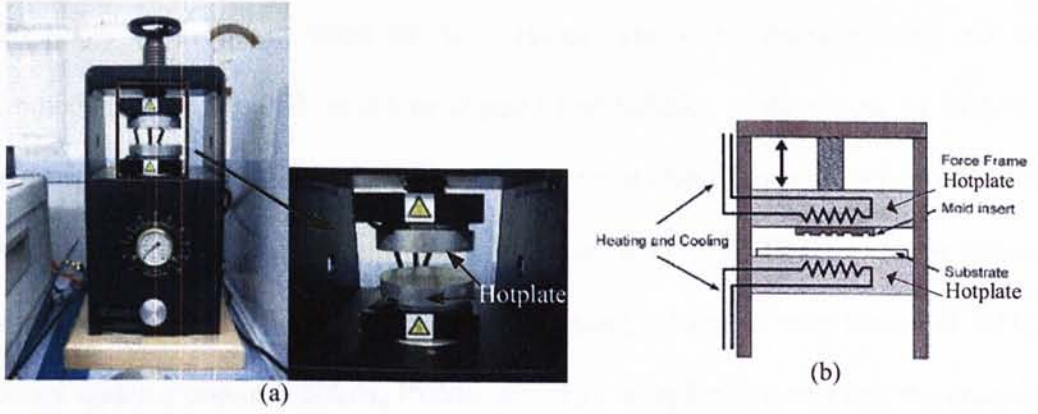

Figure 5.4 : *Hot embossing machine for compressing micro patterns on PMMA. (a) Photograph of the machine. (b) Schematic diagram of the machine.*

5.2.3 Assembly of Micropump by PDMS Bonding Process

After the micropump and the microchannel patterns were created by hot embossing technique, machining tools were used to deepen the chamber. An impeller and a DC motor were assembled on the top and the bottom of the chamber respectively. The inlet and outlet of the micropump were produced by drilling holes through another bare PMMA substrate.

The bonding of the embossed PMMA substrate and the bare PMMA substrate was achieved by spinning a layer of PDMS on the bare PMMA substrate. The assembly process of the vortex micropump is illustrated in Figure 5.5. PDMS prepolymer (SYLGARD 184 Silicone Elastomer Kit, Dow Corning) was mixed with its curing agent in the volume ratio of 10:1. Then, the prepolymer mixture was degassed in a desiccator with a vacuum pump at 50torr for half an hour to remove any bubbles created during mixing. A 10-50μm PDMS prepolymer mixture was spun on the bare PMMA surface. The size of the PMMA substrates was 2.5cm wide, 3.5cm long and 0.3cm thick. After spinning on the PDMS, the substrate was pre-cured at room temperature first for about 20 hours to evaporate most of the solvents. The two substrates were not bonded immediately because air could be trapped and bubbles could appear in PDMS layer. However, the PDMS layer was only partially cured after 20 hours. 24 hours is needed to fully cure PDMS at room temperature. This partially cured PDMS was very viscous and sticky, and was suitable for bonding. The bonded substrates were heated at 90°C for 3 hours under a pressure 50kPa. PDMS was thus completely cured and the channel was sealed. The bonded vortex micropump and the microchannel are shown in Figure 5.6.

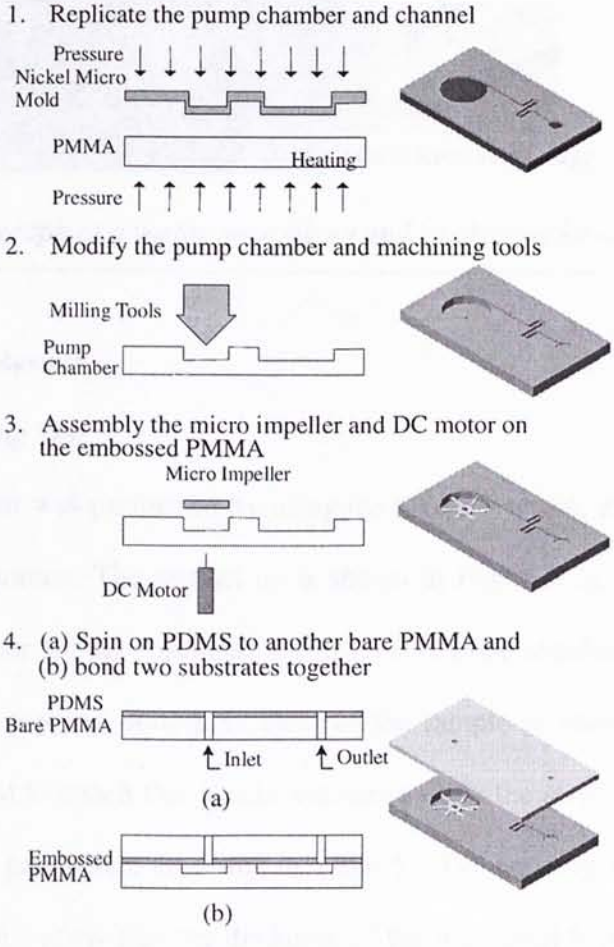

Figure 5.5 : *Replication and Assembly Processes of the vortex micropump.*

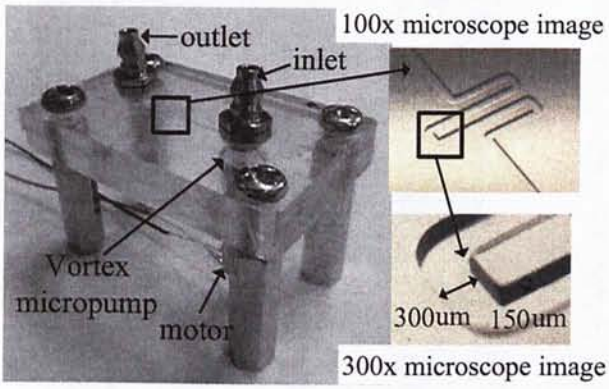

Figure 5.6 : *Photograph of a vortex micropump and its channel structure.*

5.3 Experimental Results

5.3.1 Tensile Bonding Test

The bonding test was performed by using the QTest^{TM} tensile strength tester from MTS System Corporation. The test set up is shown in Figure 5.7a. In order to fit the sample to the gripper of the machine, a piece of PMMA attachment substrate was adhered to both the top and bottom surfaces of the sample as shown in Figure 5.7b. Chloroform was used to attach this attachment substrate to the samples. The evaluation results with various parameters are listed in Table 5.1.The bonding strength was about 0.015MPa. The results show that the thickness of the interfacial layer does not greatly affect the bonding strength. However, it does affect the bonding quality. Fewer bubbles formed with a thinner PDMS layer. Besides the thickness of PDMS layer, the pre-curing time of PDMS at room temperature also has a significant influence on the bonding quality. Sufficient pre-curing time (~20 hours) is needed to reduce bubble formation and achieves a larger bonded area. A larger bonded area leads to a stronger bonding strength.

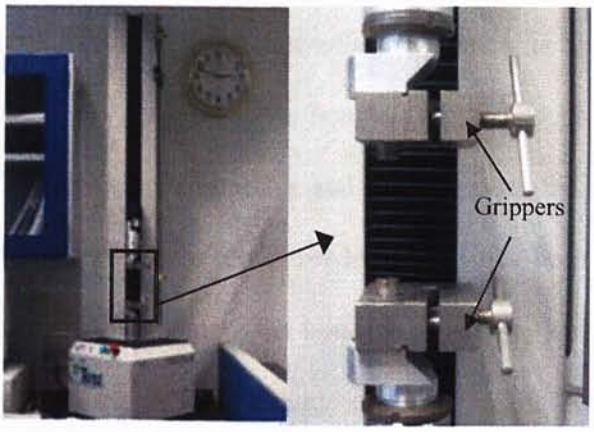

(a)

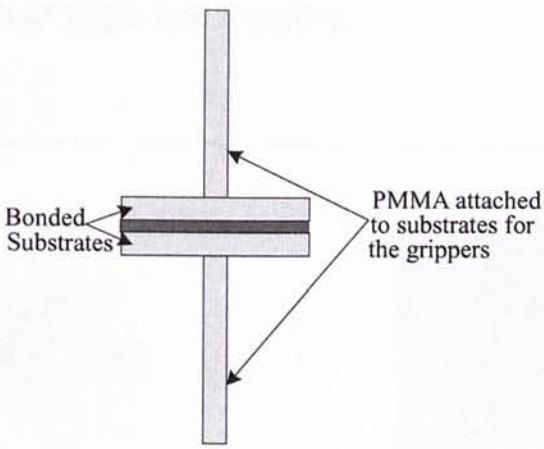

(b)

Figure 5.7 : *Experimental setup of the tensile bonding test. (a) Photograph of the QTestTM tensile testing machine. (b) Two PMMAs were mounted to the top and bottom surfaces of the bonded substrates to fit the grippers of the machine.*

Table 5.1 Evaluation results of the bonding tests.

Sample No.	PDMS thickness (μm)	Curing time at room temperature (hr)	Bonding temperature (°C)	Bonding time (hr)	Bonding strength (MPa)	Bonded area (%)	Bubbles formed
1	10	20	90	3	0.015689	100	No
2	25	20	90	3	0.015389	95	Yes
3	35	20	90	3	0.014711	95	Yes
4	10	6	90	1.5	0.011922	90	Yes
5	25	6	90	1.5	0.009900	85	Yes

5.3.2 Leakage Test

The most common concern about microfluidic system is the leakage problem. Many existing polymer-to-polymer substrate bonding methods such as gluing by epoxy or methanol suffered form uneven bonding and leakage near the edge of the device. Therefore, our fabricated device was tested for leakage. Since both PMMA and PDMS are transparent, it is difficult to examine the bonding quality by human eyes. Color dye was pumped into the channel, and no leakage occurred in the channels as shown in Figure 5.8. The channel dimensions in Figure 5.8 are w=300μm, h=100μm, l=1.6cm, and w=1mm, h=1mm, total length=2cm respectively.

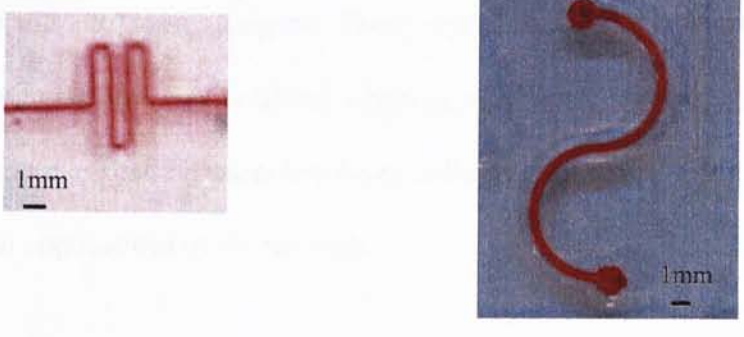

Figure 5.8 : *Color dyes were pumped into the microchannels showing that no leakage occurred. (Left) Dimensions: w=300μm, h=100μm, l=1.6cm. (Right) Dimensions: w=1mm, h=1mm, total length=2cm.*

CHAPTER SIX

DIGITAL MICROFLUIDICS IN MICROCHANNEL

Electrowetting-on-dielectric (EWOD) principle can be employed to transport micro droplets in microchannels. With specially designed microchannel, different fluidic operations such as pumping and mixing can be performed.

6.1 Digital Microfluidics

Digital Microfluidics means that the fluid flow in the device is in the form of discrete droplet rather than in continuous form. Micromechanical switch [25] and digital microfluidic circuits [26] were designed. These digital fluidic systems can be used for biotechnology applications such as lab-on-a-chip or micro total analysis system (μTAS). Drug delivery and diagnostic devices involving colloids, molecules and biological cells are also potential applications of the research.

6.2 Design of the Microchannel

Electrowetting-on-dielectric (EWOD) principle can actuate micro droplet by changing the surface tension of the dielectric layer. The micro droplet can be transported in a microchannel if a series of driving electrodes are placed inside the microchannel as shown in Figure 6.1. The electrode "on" stands for voltage applied. A photo of the driving electrodes is shown in Figure 6.2. The size of the electrode is 1mm×1mm and the material is gold. The distance between the electrodes is 50μm. The distance is small

in order to facilitate continuous movement of the droplets between adjacent electrodes. Besides transporting micro droplet, by switching on and off different driving electrodes, more advance operations such as cutting and merging of droplets can also be performed. The details are illustrated in Figure 6.3 and Figure 6.4.

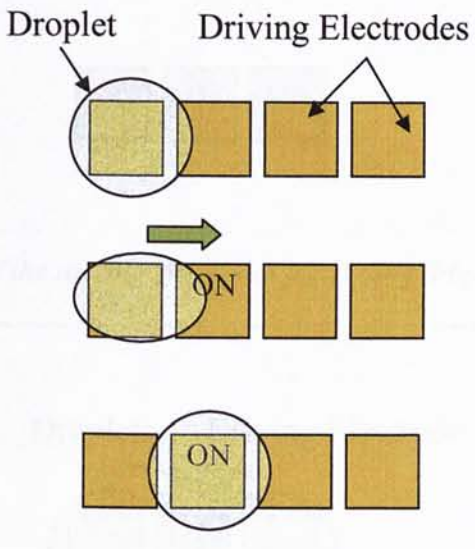

Figure 6.1 : *Design of the driving electrodes for transporting droplet.*

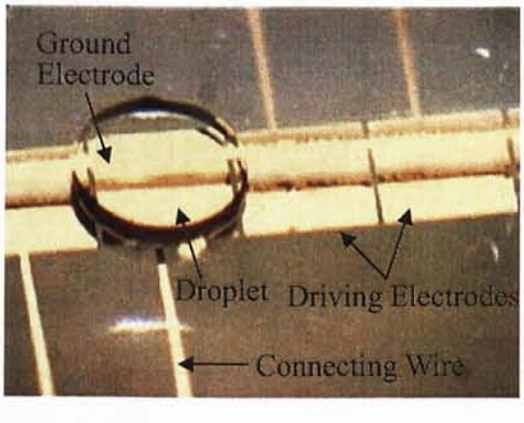

Figure 6.2 : *Photo of the gold electrodes for transporting droplet in a microchannel.*

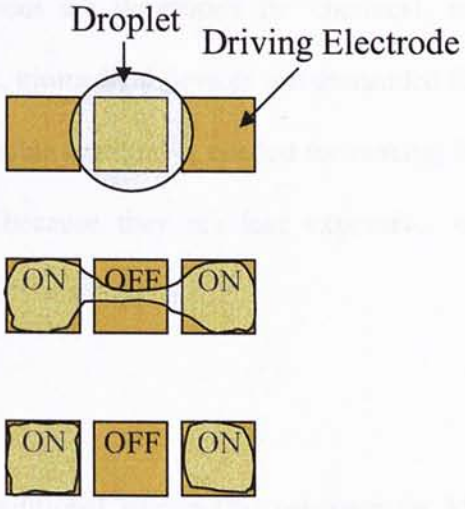

Figure 6.3 : *Design of the driving electrodes for cutting droplet.*

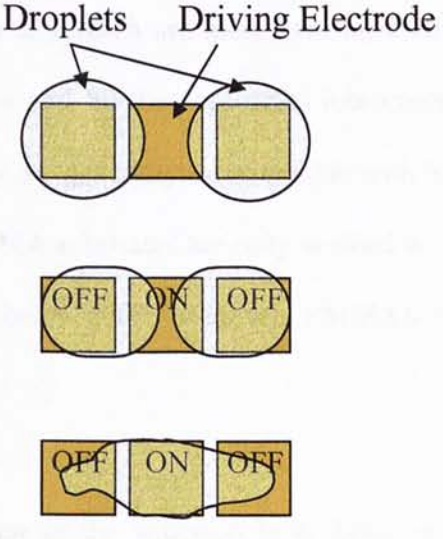

Figure 6.4 : *Design of the driving electrodes for merging droplet.*

6.3 Materials of the Microchannel

Most microfluidic devices are developed for chemical, biological, and medical applications. In recent years, biomedical devices are demanded for medical experiments and researches. A biocompatible material is needed for making these devices. Polymers become popular materials because they are less expensive, easy to fabricate, easy disposal, and biocompatible.

6.3.1 Substrate

Instead of using the traditional silicon (Si) substrate for MEMS devices, PMMA substrate is used for fabricating the device. PMMA, in contrast to Si and glass, is inexpensive. Since the structural material of the microchannel is another polymer, PMMA can have a better adhesion. The PMMA substrates used in this project is 0.2mm thick. The disadvantages of PMMA are more care must be taken to control its surface chemistry than with glass and Si; they are often inbiocompatible with organic solvent such as acetone; and they are generally incompatible with high temperatures. Therefore, unlike Si substrates, PMMA substrates are only washed with IPA and DI water. All the fabrication processes are below 100°C to prevent PMMA substrates from melting.

6.3.2 Adhesion Layer

Parylene C is chosen as the adhesion layer between the PMMA substrate, gold electrodes, and PDMS layer. The details are explained in Chapter four. Another advantage of using parylene C is its transparent property. The whole microchannel needs to be transparent in order to observe the microchannel. The thickness of parylene C is

~0.3μm.

6.3.3 Electrode

Gold (Au) and platinum (Pt) are usually the materials of electrode in MEMS devices. In this project, Gold (Au) is used as the material of both the ground and driving electrodes. Indium-tin-oxide (ITO) is an ideal material for making electrodes because it is transparent. However, because of the fabrication problem (Details are discussed in Chapter four); ITO cannot be used in this project. The width of Au ground electrodes need to be decreased (~200μm) so that the inside of the microchannel can still be observed.

6.3.4 Dielectric Layer

Polydimethylsiloxane (PDMS) is chosen as the dielectric layer and structural material of the microchannel. PDMS is an elastic polymer that can be fabricated easily using soft lithography. It cures at low temperature (around 65°C for 4 hours). It is hydrophobic, so no additional layer is needed to make the surface hydrophobic. EWOD can take place on PDMS directly. It is nontoxic and biocompatible; cells and proteins can be cultured directly on it. For microfluidic devices, sealing is a great concern. PDMS can seal reversibly to itself and a range of other materials by making van der Waals contact with the surface, or it can seal irreversibly after exposing to oxygen plasma by formation of covalent bonds (Detailed are discussed in Chapter three.). The characteristics of PDMS [28], Teflon [29], and parylene C [30] are compared in Table 6.1. The dielectric constant of PDMS is approximately the same as Teflon and parylene

C. The dielectric breakdown voltage of PDMS is the same as Teflon. However, parylene C has a relatively small dielectric breakdown voltage. The larger the dielectric breakdown voltage, the less chance electrolysis will occur.

Table 6.1 Electrical properties of PDMS, Teflon, and parylene C.

Material	PDMS	Teflon	Parylene C
Dielectric Constant	2.75	1.93	3.10
Dielectric Strength (kV/mm)	21	21	5.6

6.4 Fabrication of the Microchannel

The photos of the two layers are shown in Figure 6.5. The fabrication process of the microchannel is illustrated in Figure 6.6. The microchannel is divided into top and bottom layers. The top layer contains the ground electrode and the bottom layer contains the driving electrodes. The details of the fabrication process are discussed in Chapter three and Chapter four. The two layers are finally sealed to form the closed microchannel.

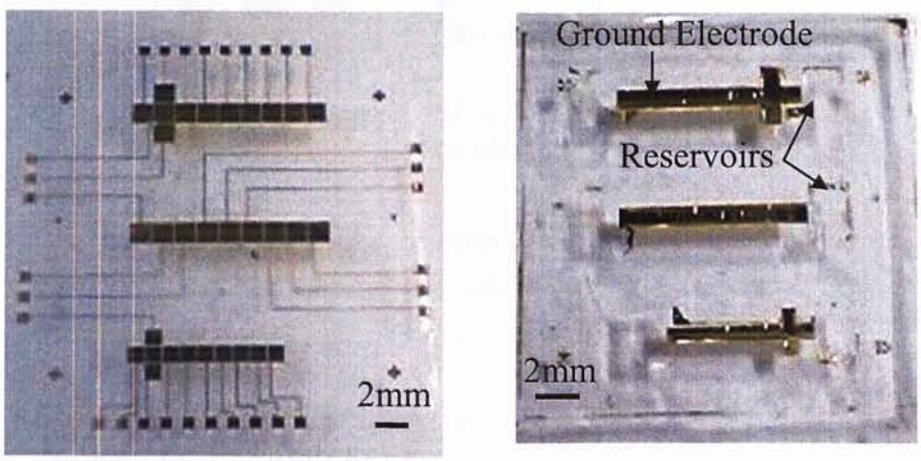

Figure 6.5 : *Photos of the (left) top and (right) bottom layers.*

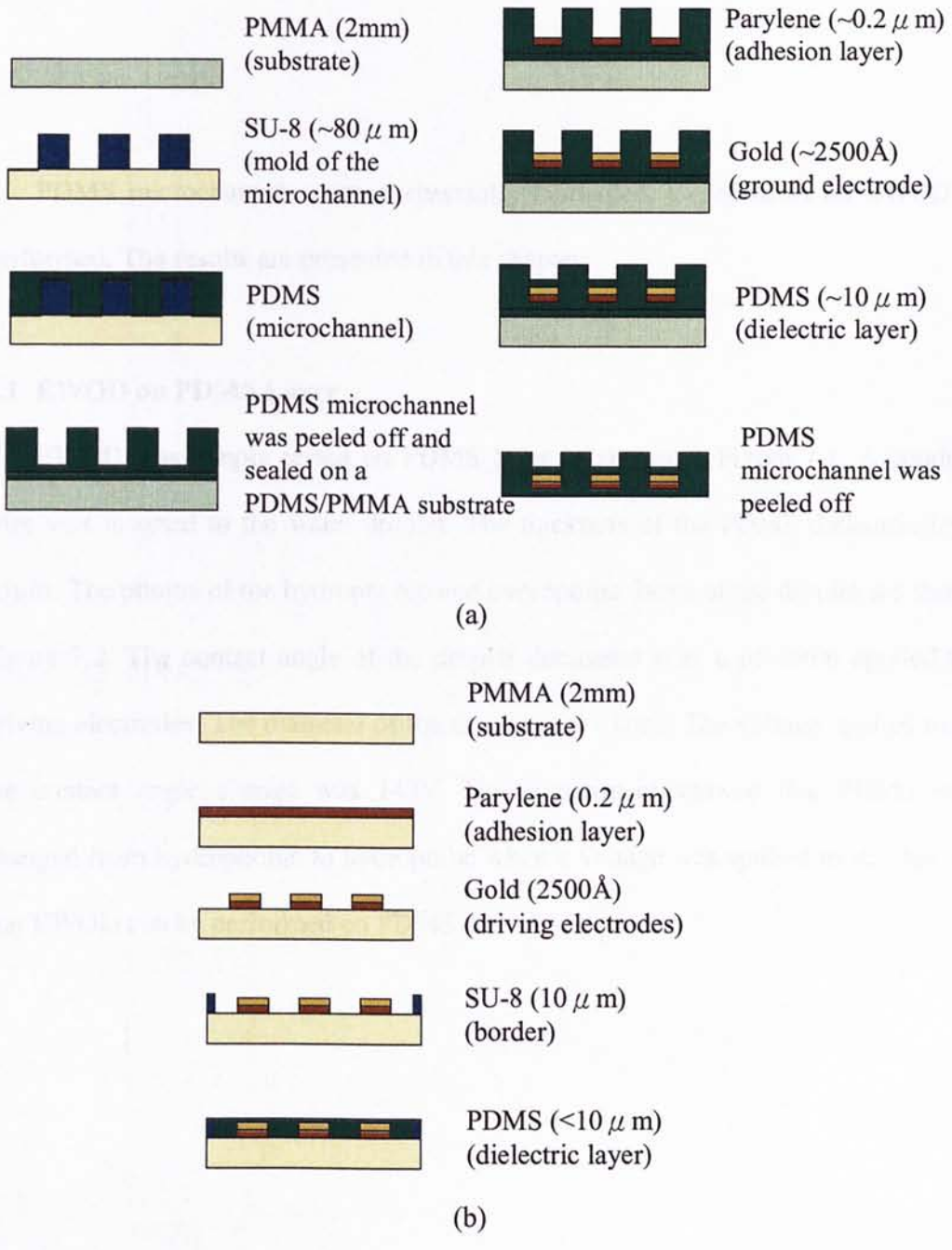

Figure 6.6 : *Fabrication process of the microchannel. (a) Top layer. (b) Bottom layer.*

CHAPTER SEVEN

EXPERIMENTAL RESULTS

PDMS microchannels were successfully fabricated. Experiments on EWOD were performed. The results are presented in this chapter.

7.1 EWOD on PDMS Layer

EWOD was simply tested on PDMS layer as shown in Figure 7.1. A conducting wire was inserted to the water droplet. The thickness of the PDMS dielectric layer is ~5μm. The photos of the hydrophobic and hydrophilic forms of the droplet are shown in Figure 7.2. The contact angle of the droplet decreased after a potential applied to the driving electrodes. The diameter of the droplet was ~1mm. The voltage applied to make the contact angle change was 145V. This experiment showed that PDMS surface changed from hydrophobic to hydrophilic when a voltage was applied to it. This shows that EWOD can be performed on PDMS dielectric layer.

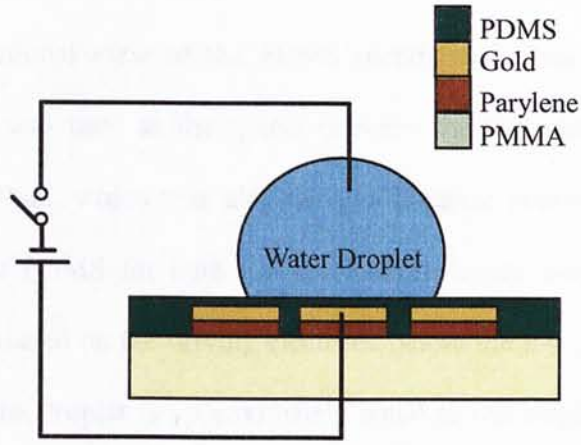

Figure 7.1 : *Schematic configuration of EWOD demonstration on PDMS.*

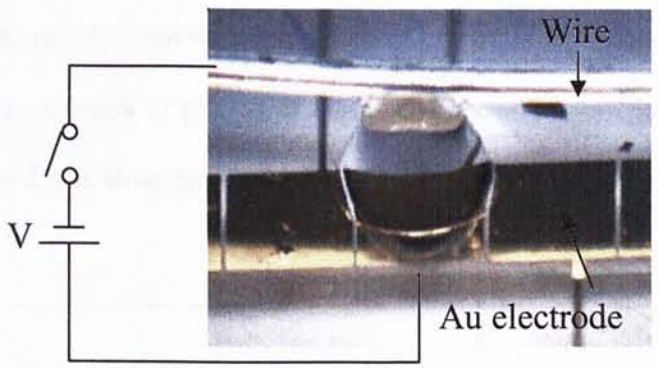

(a)

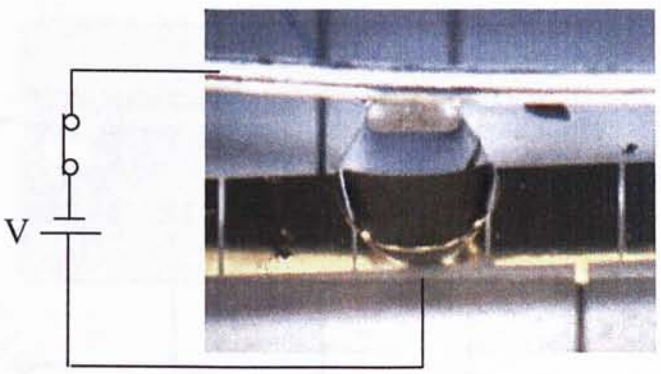

(b)

Figure 7.2 : *Photos of basic EWOD demonstration on PDMS. (a) Droplet in hydrophobic condition. (b) Droplet in Hydrophilic condition.*

7.2 PDMS Parallel Plate Channel

The cross-sectional view of the PDMS parallel plate microchannel is shown in Figure 7.3. SU-8 was used as the spacer between the two plates. The thickness was approximately 300μm, which was also the gap distance between the two plates. The thicknesses of the PDMS for both top and bottom layers were ~10μm. A DI water droplet was first placed on the driving electrode before the top plate was covered on it. The diameter of the droplet is approximately equal to the length of the electrode, i.e., 1mm. Then, a positive potential (~220V) was applied to the adjacent electrode. This made the contact angle of the droplet at the end region change. Movement of droplet was initiated. The droplet moved to the adjacent electrode in 10 minutes. The distance moved was 1mm. A series of photos in Figure 7.4 show the movement of the droplet. However, the speed was slow. Several parameters were adjusted to increase the speed.

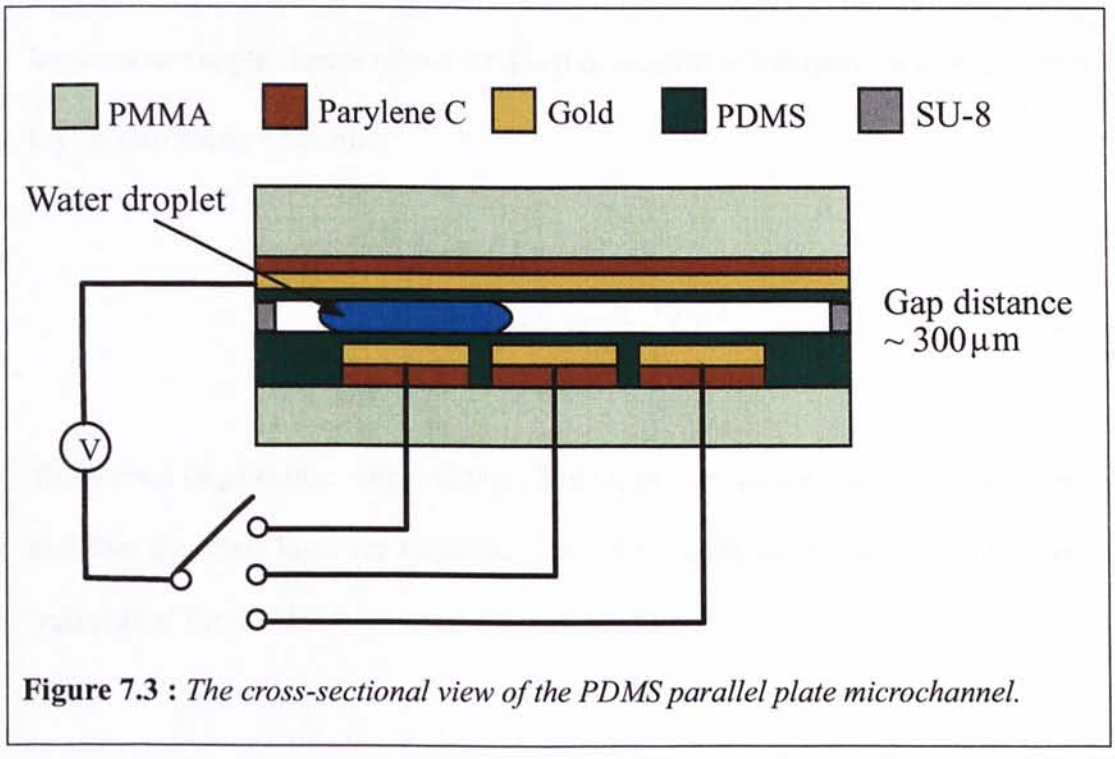

Figure 7.3 : *The cross-sectional view of the PDMS parallel plate microchannel.*

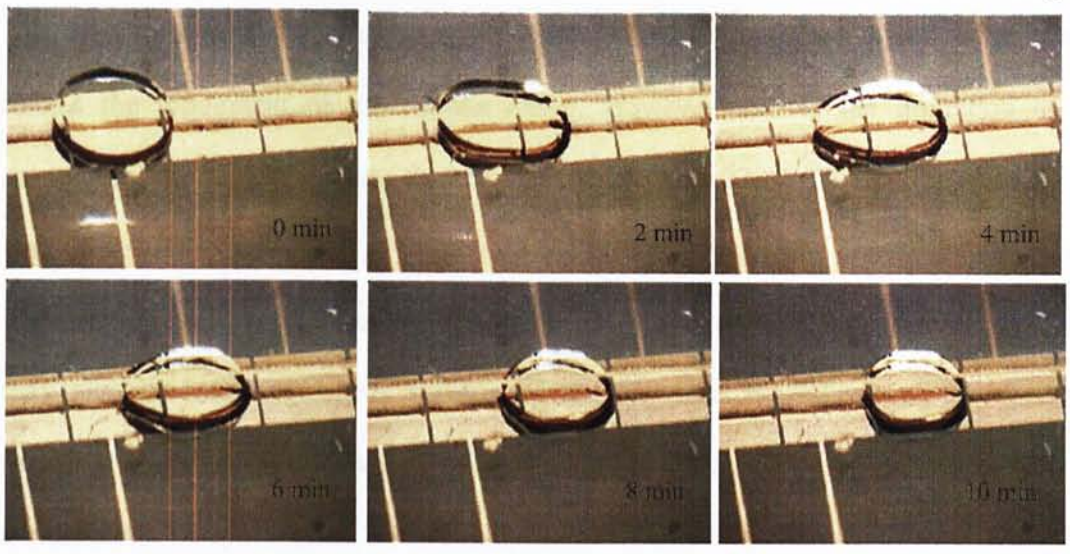

Figure 7.4 : *Captured images for droplet transport in the parallel plate microchannel.*

7.2.1 Contact Angle

One of the factors that affect the speed of the droplet is the contact angle change. A large contact angle change (about 40° [31]) is required to transport the droplet. From the Lippmann-Young's equation:

$$\cos\theta = \cos\theta_0 + \frac{1}{\gamma_{LG}}\frac{1}{2}CV^2 \qquad \text{Eq. 7.1}$$

To obtain a large contact angle change, large applied potential, large dielectric constant, and thin dielectric layer are required. These parameters were modified to improve the transport of the droplet.

7.2.1.1 Applied Potential

According to Eq. 7.1, a larger voltage leads to a large contact angle change, which makes the movement of the droplet easier. However, due to the limitation of the equipment, the largest voltage that can be applied was 220V. This voltage could only lead to a small contact change and could not further increase the contact angle change. The droplet could not be moved in high speed. Moreover, a very large applied voltage may also lead to electrolysis because of the electrical breakdown of the dielectric material. Therefore, it may not be a good method to increase the contact angle change of the droplet.

7.2.1.2 Dielectric Thickness

The thickness of the dielectric layer should be as small as possible, down to several microns or even less. However, the thinnest PDMS dielectric layer that could be made was only ~5μm. Those thinner than 5μm were difficult to cure during the fabrication process. From the experimental results, only those samples that had a PDMS layer thinner than 10μm could be transported in the microchannel in a slow speed. For those that had a PDMS layer greater than 10μm, only a very small contact angle change was achieved and the droplet could not be moved. This shows that the PDMS thickness affects the contact angle change. From these results, it can be predicted that if the thickness of PDMS is decreased down to ~1μm or less, the contact angle change can be increased. Hence, the speed of the droplet can also be increased.

From Eq. 7.1, V_d does not represent the applied voltage, it is the voltage across the bottom layer. In the experiments, the total voltage applied was divided across the top and

bottom layers depending on the capacitance of the dielectric layers. If the thicknesses of the PDMS layer for both top and bottom layers are the same, the contact angle changes would also be the same. This would make the movement of the droplet difficult. Therefore, by designing different thickness to the top and bottom layers, different contact angle change can be obtained. The thickness of the PDMS layer of the top layer is greatly reduced (<1μm), the voltage drop across it can be negligible. All the applied voltage would drop across the bottom layer and enhance the movement of the droplet.

7.2.1.3 Ground Electrode

For the convenience to observe the microchannel, the width of the ground electrode was decreased to 200μm. After the testing experiments, the ground electrode was widened to see if it affects the movement of the droplet. Microchannels with different widths of the ground electrode are shown in Figure 7.5. Nevertheless, the wider ground electrode did not improve the situation.

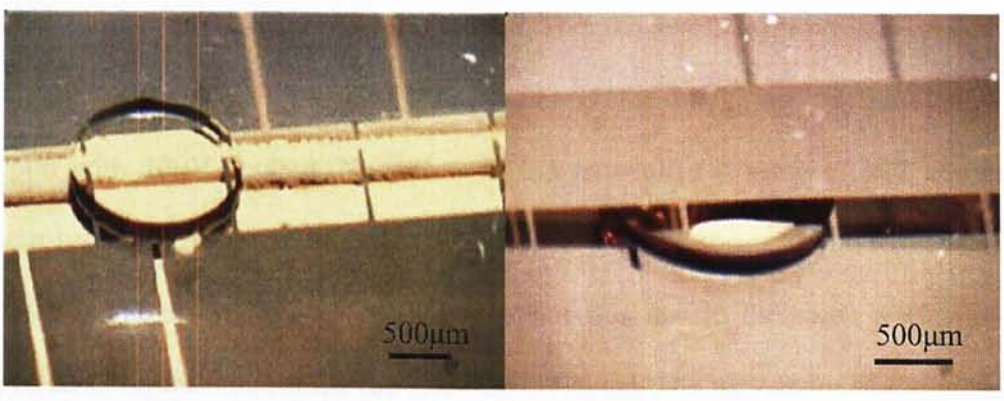

Figure 7.5 : *Photos of microchannels with different widths of the ground electrode. (a) The width is 200μm. (b) The width is 1mm.*

7.2.1.4 Gap Distance

From the derivation of the cutting droplet, the channel gap distance d is inversely proportional to the difference of contact angles. With a small channel gap, a large contact angle change can be obtained. By adjusting the thickness of the SU-8 spacer, the channel gap was decreased to ~70μm. The experimental results showed that there was only a slight improvement.

7.3 Parylene C Parallel Plate Channel

Since the thickness of the PDMS dielectric layer could not be decreased to <5μm, parylene C replaced PDMS as the dielectric layer. The dielectric constants of parylene C and PDMS are very close. Thin layers (<1μm) of parylene C can be deposited by Specialty Coating Systems. EWOD experiments similar to the one described above were performed on 500Å and 2000Å thick parylene C layers.

For the 500Å thick parylene C microchannel, only 30V was needed to actuate the droplet, i.e., with a change in contact angle. However, no motion of the droplet was observed. Then, the voltage was gradually increased to 220V. After 2 seconds, electrolysis occurred as shown in Figure 7.6. The parylene C layer broke down.

For the 2000Å thick parylene C microchannel, the droplet was initiated to move in 1 second with 100V applied. Nevertheless, the movement stopped after 2 seconds. No electrolysis occurred even with 220V applied for over 30 seconds. The movement of the droplet is shown in Figure 7.7. The problem was due to the same thickness of the parylene C layers on both the top and bottom layers. The movement of the droplet was locked by the same contact angle change at the top and bottom of the droplet. This

problem can be solved by depositing a very thin parylene C layer on the top layer. Then, the contact angle change at the top of the droplet can be very small or negligible.

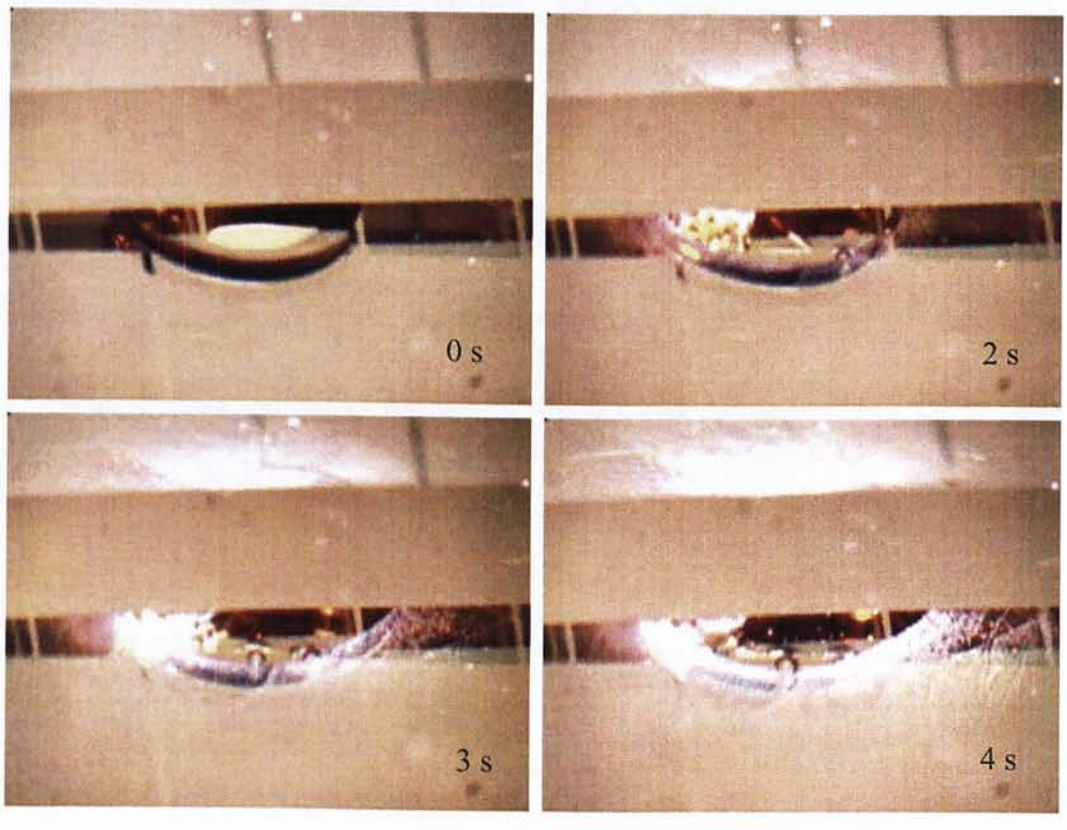

Figure 7.6 : *Photos of electrolysis occurred in 500Å thick parylene C microchannel.*

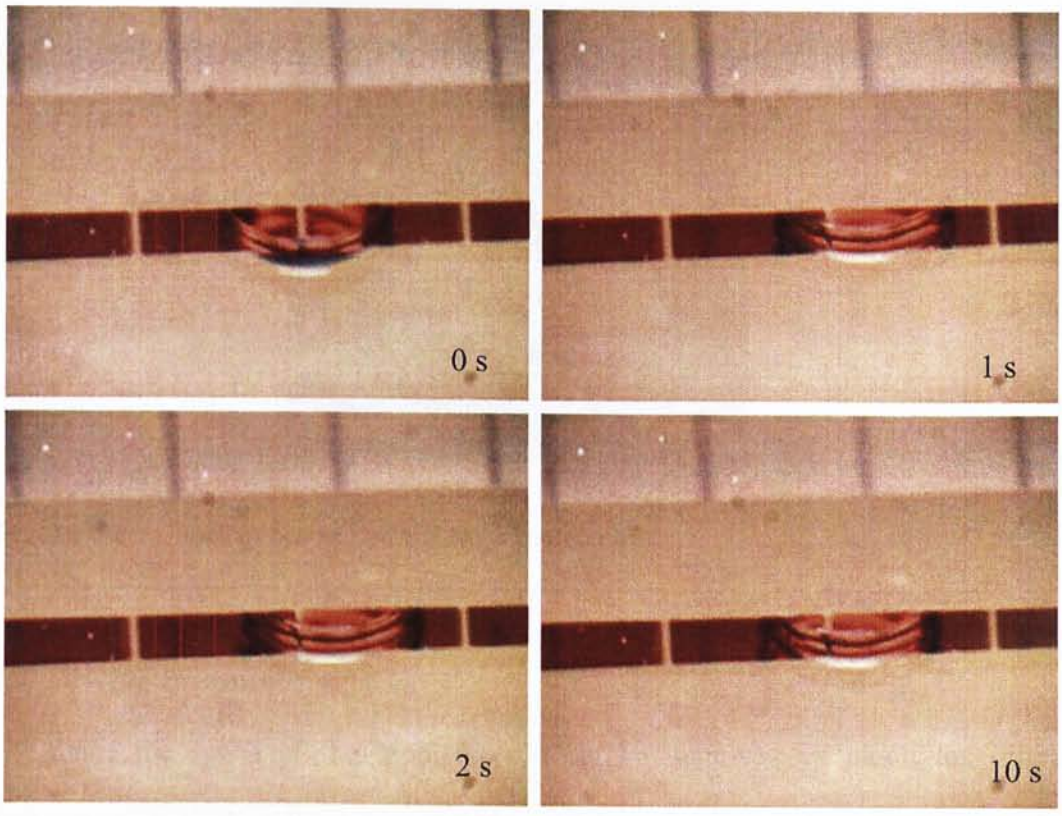

Figure 7.7 : *Photos of droplet movement in 2000Å thick parylene C microchannel.*

7.4 Sealed PDMS Microchannel

Sealed PDMS microchannel was also tested with EWOD experiment. The photo of the sealed PDMS microchannel is shown in Figure 7.8. The channel gap was 70μm.The two reservoirs were opened and the liquid was placed in one of them. The first electrode was then activated. The liquid was attracted into the channel. The speed was very slow as the PDMS layer was thick (~10μm). This experiment showed that liquid could be pumped into the microchannel by EWOD without using micropumps and microvalves.

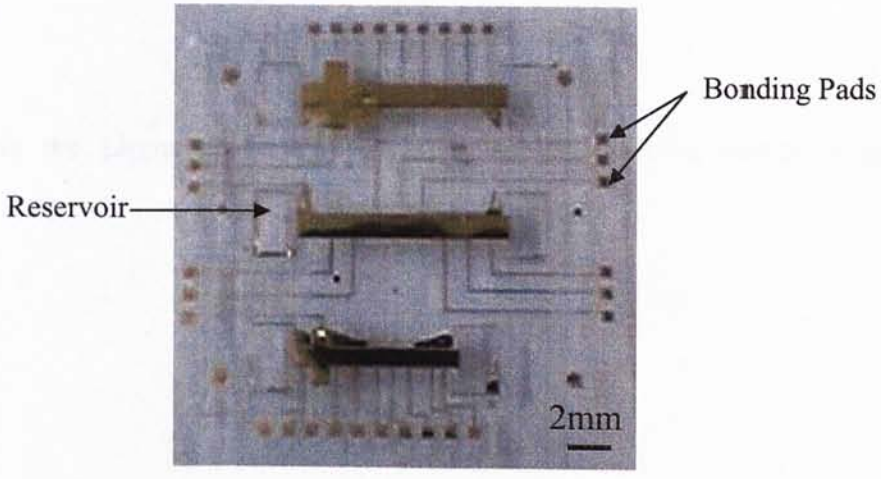

Figure 7.8 : *Photo of the sealed PDMS microchannel.*

7.5 Driving Pressure

Since the speed of the droplet could not be improved by modifying different parameters, a mathematical approach is used to estimate the driving pressure of the droplet. A schematic for the driving mechanism is shown in Figure 7.9. The pressure at the left and right menisci of the liquid is expressed as follows [32]:

$$p_L - p_a = -\frac{\gamma_{LG}}{d}(\cos\theta_t + \cos\theta_{b0}) > 0 \qquad \text{Eq. 7.2}$$

$$p_R - p_a = -\frac{\gamma_{LG}}{d}(\cos\theta_t + \cos\theta_b) < 0 \qquad \text{Eq. 7.3}$$

where p_L, p_R, and p_a are the pressures of the left, right of the menisci and air respectively.

The difference between the left and right sides of the liquid is the driving pressure for the motion of the liquid droplet.

$$\Delta p = p_L - p_R = \frac{\gamma_{LG}}{d}(\cos\theta_b - \cos\theta_{b0}) \qquad \text{Eq. 7.4}$$

Using the Lippmann-Young's Eq. 7.1, Eq. 7.4 can be further simplified to Eq. 7.5.

$$\Delta p = \frac{1}{2d}CV^2 = \frac{\varepsilon_0 \varepsilon V^2}{2dt} \qquad \text{Eq. 7.5}$$

where ε_0 (8.854×10^{-12} C/V) is permittivity of vacuum, ε is the dielectric constant of the dielectric layer, V is the applied voltage, d is gap size, and t is the thickness of the dielectric layer.

By substituting the parameters of the PDMS parallel plate channel into Eq. 7.5, the driving pressure of the motion of the water droplet can be estimated. The dielectric constant of PDMS is 2.75, applied voltage is 220V, gap size is 300μm, and thickness of PDMS is 5μm.

$$\Delta p = \frac{(8.854\times10^{-12})(2.75)(220)^2}{2(300\times10^{-6})(5\times10^{-6})} = 392.8Pa$$

Compare with the results of other groups, the driving pressure of a Teflon microchannel is ~9kPa [32]. This shows that the driving pressure of the PDMS microchannel is not large enough and leads to the slow speed of the droplet.

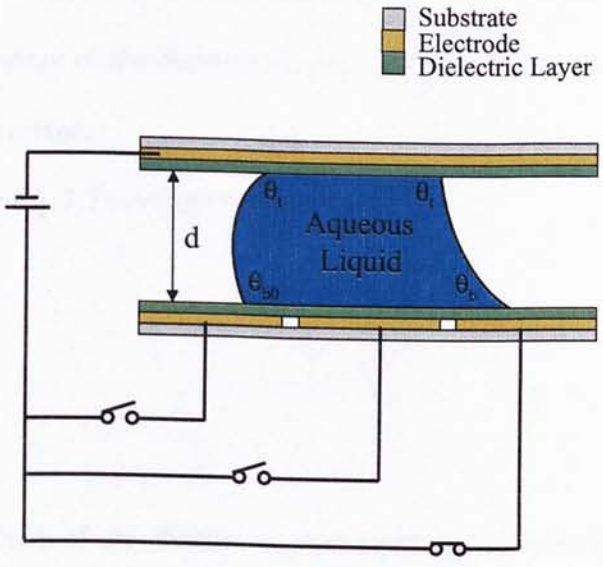

Figure 7.9 : *Driving mechanism of the microchannel.*

7.6 Microchannel in the Vertical Position

In order to find out whether the microchannel can be operated in the vertical position, the electrowetting force and gravitational force are considered. The force analysis of the droplet is shown in Figure 7.10. The electrowetting force γ_{EW} is the electrostatic force produced by the applied voltage across the top and bottom plates of the microchannel, which modifies the interfacial surface tension. It can be expressed by Eq. 7.6 [33]:

$$\gamma_{EW} = \frac{1}{2}\frac{t}{\varepsilon_0 \varepsilon}\sigma_L^2 \qquad \text{Eq. 7.6}$$

$$\sigma_L = \frac{\varepsilon_0 \varepsilon V}{t} \quad \text{(Gauss' law)} \qquad \text{Eq. 7.7}$$

where σ_L is the charge density of the liquid phase, ε_0 is the permittivity of vacuum, ε is the dielectric constant of the dielectric layer, t is the thickness of the dielectric layer, and V is the applied voltage.

Substituting Eq. 7.7 into Eq. 7.6 gives

$$\gamma_{EW} = \frac{1}{2}\frac{\varepsilon_0 \varepsilon V^2}{t} \qquad \text{Eq. 7.8}$$

The parameters of the PDMS microchannel are substituted into Eq. 7.8. ε=2.75, V=220, and t=5μm. The electrowetting force γ_{EW} of the PDMS microchannel is 0.1178N.

The gravitational force of the water droplet is calculated as follows:

$$W=mg \qquad \text{Eq. 7.9}$$

Diameter of the water droplet = 1mm

Volume of the water droplet $= \frac{4}{3}\pi(0.05)^3 = 0.000523cm^3$

Mass of the water droplet = 0.000523g = 5.23×10^{-7} kg

W = $(5.23\times10^{-7})(9.81) = 5.13\times10^{-6}$ N

From the above calculation, it shows that the electrowetting force produced by the applied voltage is much greater than the gravitational force. It can be concluded that the microchannel can be operated at the vertical position.

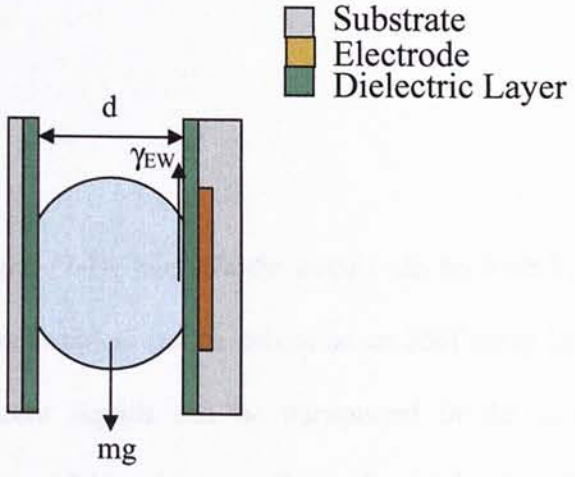

Figure 7.10 : *The force analysis of the microchannel at the vertical position.*

CHAPTER EIGHT

FUTURE WORK

A complex two dimensional (2-D) microfluidic circuit can be built by combining several microchannels together. Droplets can be driven on an X×Y array by controlling the driving electrodes. Different liquids can be transported in the microchannels. Chemical mixing can be performed by merging different liquid droplets. This chapter discusses the feasibility of accomplishing the above task.

8.1. Digital Microfluidic Circuit Design

Droplet transportation was successfully performed by EWOD in a single microchannel. A number of microchannels can be integrated in two dimensions. This makes the droplet transport in two directions. The conceptual design of the circuit is shown in Figure 8.1.

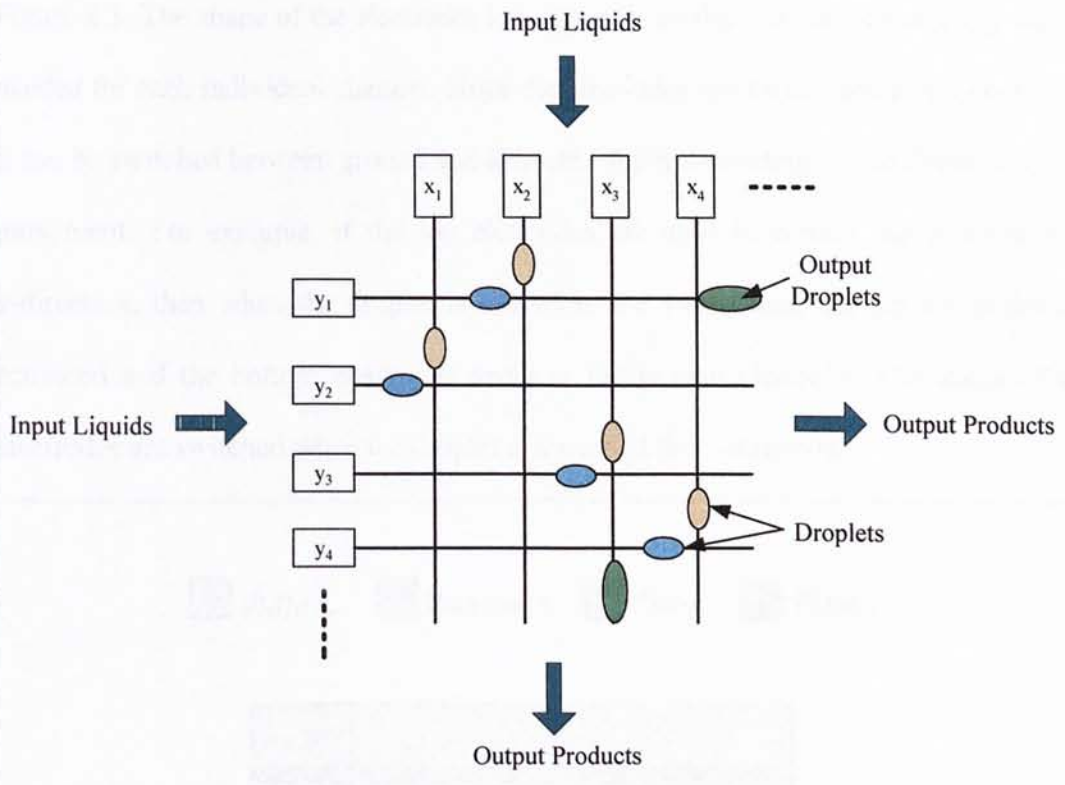

Figure 8.1 : *Conceptual description of digital microfluidic circuit.*

8.1.1. Electrodes Design

Since the droplet is transported in two directions, the electrode patterns become complicated. Each electrode is connected to an individual bonding pad for voltage applied. As the number of electrode increases, the number of connecting wires also increases. It is difficult to connect the electrodes in the middle of the array because there is no space for the connecting wire. The circuit becomes very complicated. The electrodes have to be designed with another approach.

The top and bottom electrodes are divided into two sets of electrode. One set is used to control the movement of the droplet in x-direction, where the other set is used to

control the movement in y-direction. The proposed design is shown in Figure 8.2 and Figure 8.3. The shape of the electrodes is a rectangle so that only one connecting wire is needed for each individual channel. Since the electrodes can be independently controlled, it can be switched between ground and activated states depending on the direction of the movement. For example, if the top electrodes are used to control the movement in y-direction, then when the droplet is moved in the y-direction, the top electrodes are activated and the bottom electrodes serve as the ground electrode. The states of the electrodes are switched when the droplet is moved in the x-direction.

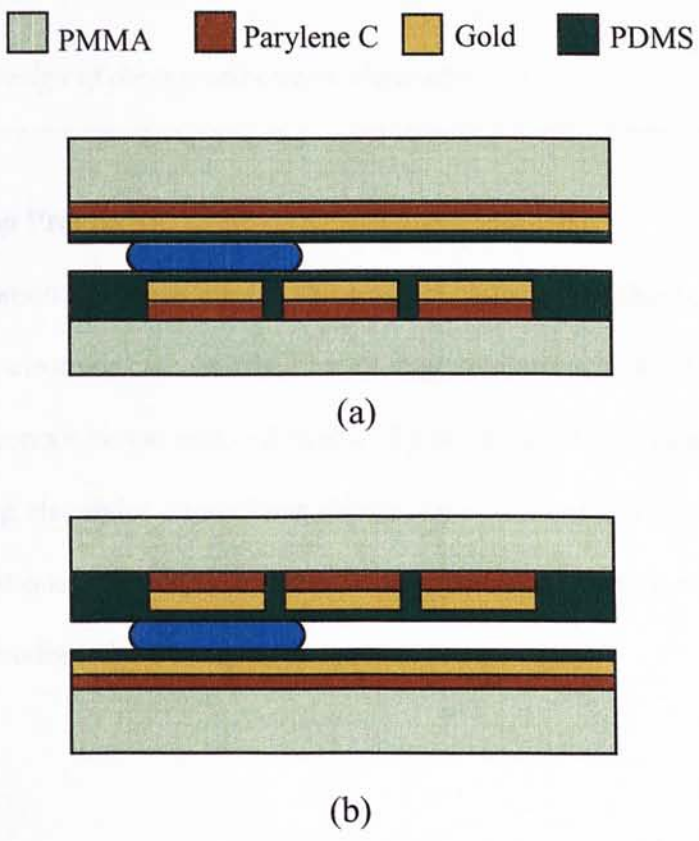

Figure 8.2 : *Cross-sectional view of the microfluidic circuit. (a) From the x-direction. (b) From the y-direction.*

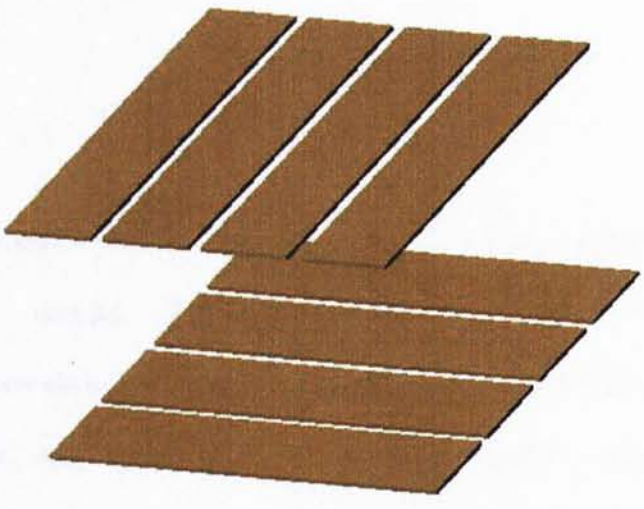

Figure 8.3 : *Design of the top and bottom electrodes.*

8.2. Fabrication Process

The fabrication processes are the same as the single microchannel. Since both the top and bottom electrodes are switched between ground and activate states, the width of the electrodes cannot be too thin (~200μm), like the design of the single microchannel. The thin driving electrodes do not have enough force to move the droplet. However, by using gold electrodes, the inside of the channels will be blocked. It is better to change one of the electrodes to be a transparent material such as ITO.

CHAPTER NINE

SUMMARY

A novel method was developed to fabricate PDMS microchannel to manipulate micro liquid droplet. The ultimate goal of this research is to use electrowetting-on-dielectric (EWOD) principle, micro liquid droplet can be pumped, transported, cut, and merged in the microchannel without using any micropump and microvalves. This method does not require the fabrication of complex mechanical structures, i.e., only gold electrodes are needed. By applying potential to the driving electrodes, the charges and dipoles on the dielectric layer and in the liquid droplet redistribute, modifying the surface energy at the interface. The contact angle at the liquid-dielectric layer interface decreases, leading to a movement of the liquid droplet inside the microchannel.

PDMS was chosen as the dielectric layer of the microchannel because it is transparent, biocompatible, and permeable to gases. Microchannels were fabricated by soft lithography method. A novel fabrication method of depositing gold on PDMS was developed. Gold is difficult to deposit on PDMS because of the poor adhesion between metal and polymer. This problem was solved by using parylene C as the adhesion layer. The microchannels are 1cm long, 1mm wide, and 70μm deep. Each driving gold electrodes is 1mm×1mm in dimensions. The microchannels were finally sealed with oxygen plasma as PDMS could be reversibly sealed with this method.

Experimental results showed that water droplet could be transported in the parallel

plate microchannel. However, because of the limitation of the fabrication process, the thinnest PDMS layer that could be made was only 5μm. This caused the contact angle change of the droplet not large enough to transport the droplet in high speed. The droplet moved 1mm distance in 10 minutes. Different parameters such as size of electrodes and gap distance were modified to increase the speed. No significant improvements were observed. Parylene C was also used as the dielectric layer because its dielectric constant is very close to PDMS. Microchannels with 500Å and 2000Å thick parylene C were tested. Electrolysis occurred with the 500Å thick parylene C microchannel. The parylene C layer was too thin and broke down. Movement of the droplet in the 2000Å thick parylene C microchannel was initiated in 1 second with 100V applied to the driving electrode. Water was successfully pumped into the sealed PDMS microchannel by activate the first driving electrode of the microchannel.

Besides using PDMS as the structural material of the microchannels, PDMS can also be used as the bonding interface of polymer substrates. A novel bonding technique was developed to bond two PMMA substrates together. Microchannels were fabricated on PMMA substrates by hot embossing technique. Then, PDMS was spun on the bare PMMA substrate and bonded to the embossed PMMA substrate. The bonded substrates were cured at 90°C for 3 hours with an applied pressure 50kPa. Microchannel and micropump were successfully fabricated with this method.

This dissertation work has demonstrated that digital microfluidics can be performed in PDMS microchannels. Base on this microchannel, future development can be focused on developing a more complex digital microfluidic circuit, which can perform transporting, cutting, and merging of droplets. The potential applications of this device

are drug delivery, cell and DNA manipulation, and chemical mixing.

APPENDIX A

Fabrication Process

I. Sealing of the Microchannel

1. Bond both bottom and top layers.
    - Expose to O_2 plasma for 30" at 70W, 4mT separately.
    - Drop ethanol on both surfaces to provide smooth movement for manual alignment.
    - Evaporate ethanol on 80°C hot plate for 2'.

II. Process for Making SU-8 Master

1. PMMA substrate cleaning.
    - Dip in IPA for 2' (acetone may attack the substrate material).
    - DI rinse for 2'; blow dry.
2. Photolithography of the mask.
    - Dispense approximately 1ml of SU-8 (2075) resist for a 3cm×3cm substrate.
    - Wait 1' to let the resist be at rest on the substrate. Remove air bubbles if any.
    - Spin on the resist at 500rpm for 15" first and then 3000rpm for 60". (The resist needs to be spun at two stages since the viscosity of the material is so high.)
    - Soft bake on 80°C hotplate for 30'.
    - UV exposure with mask for 90".

- Post expose bake on 50°C hotplate for 20'.
- Develop in SU-8 developer for 3'.
- Rinse with IPA; blow dry. (If a white film is produced during rinse, this is an indication that the substrate has been under developed. Simply immerse or spray the substrate with SU-8 developer to remove the film and complete the development process. Repeat the rinse step.)

III. Process for Making Chromium Mask

1. Glass and transparency mask cleaning.
   a. The glass should be cleaned with acetone, IPA, and DI water.
      - Dip in acetone for 2'.
      - Dip in IPA for 2'.
      - DI rinse for 2'; blow dry.
   b. The transparency mask should be cleaned with DI water only.
2. Stick the transparency mask onto the glass with tape.
3. Stick the unpatterned chromium mask to the glass with tape.
4. Photolithography of the mask.
      - UV exposure for 30".
      - Develop in AZ5214 developer for 5'.
      - DI rinse; blow dry.
5. Etch Cr.
      - Cr (commercial) etchant for ~5'.
6. Photoresist cleaning.

- Dip in acetone for ~3'.
- Dip in IPA for ~2'.
- DI rinse; blow dry.

IV. Process for Fabricating the Bottom Layer

1. PMMA substrate cleaning.
   - Dip in IPA for 2' (acetone may attack the substrate material).
   - DI rinse for 2'; blow dry.
2. Deposit adhesion layer.
   - 2000Å parylene.
   - 0.2g parylene dime powder may produce 0.2μm thick film.
3. Sputter metal for driving electrodes, wires, and pads.
   - 2500Å Au.
4. Photolithography of the 1st mask.
   - Spin on AZ5214 photoresist at 4000rpm for 30".
   - Prebake on 75°C hot plate for 40".
   - UV exposure with mask for 60".
   - UV lamp: 350W/cm^2.
   - Develop in AZ300K developer solution for 1'.
   - DI rinse; blow dry.
5. Etch Au driving electrodes.
   - KI:I_2:DI of 10g:2.5g:200ml for 2'.
   - DI rinse; blow dry.

6. Photoresist cleaning.
    - Strip resist using acetone.
    - O_2 plasma clean for 5' at 20W, 4mT.
7. Photolithography of the 2nd mask (SU-8 border).
    - Spin on SU-8 (2015) at 3000rpm for 40".
    - Prebake on 80°C hot plate for 30'.
    - UV exposure with mask for 90".
    - Postbake on 50°C for 20'.
    - Develop in SU-8 Developer solution for 1'.
    - Rinse with IPA; blow dry.
8. Prepare dielectric layer.
    - Mix PDMS prepolymer and its curing agent at 4:1 volume ratio.
    - Degas the mixture at 50mT for 30'.
9. Deposit dielectric layer.
    - Spin on PDMS mixture at 3500rpm for 40".
    - Cure in 80°C oven for 4 hours.
10. Pattern dielectric layer.
    - Peel off the PDMS beyond the SU-8 border.

V. Process for Fabricating Top Layer

1. PMMA substrate cleaning.
    - Dip in IPA for 2' (acetone may attack the substrate material).
    - DI rinse for 2'; blow dry.

2. Photolithography of the 1st mask.
    - Spin on SU-8 (2075) at 3000rpm for 60".
    - Prebake on 80°C hot plate for 40'.
    - UV exposure with mask for 90".
    - Postbake on 50°C hot plate for 20'.
    - Develop in SU-8 Developer solution for 2'.
    - Rinse with IPA; blow dry.
3. Prepare structural material.
    - Mix PDMS prepolymer and its curing agent at 10:1 volume ratio.
    - Degas the mixture at 50mT for 30'.
4. Deposit structural material.
    - Spin on PDMS mixture at 500rpm for 60".
    - Cure in 80°C oven for 2 hours.
    - Peel off PDMS from the SU-8 mold.
5. PMMA substrate cleaning.
    - Dip in IPA for 2' (acetone may attack the substrate material).
    - DI rinse for 2'; blow dry.
6. Prepare adhesion layer.
    - Mix PDMS prepolymer and its curing agent at 10:1 volume ratio.
    - Degas the mixture at 50mT for 30'.
7. Deposit adhesion layer.
    - Spin on PDMS mixture at 3000rpm for 40".
    - Cure in 80°C oven for 2 hours.

8. Bond structure polymer to PMMA+PDMS substrate for further fabrication processes.
    - Expose to O_2 plasma for 30"at 70W, 4mT separately.
    - Drop ethanol on both surfaces to provide smooth movement for manual alignment.
    - Evaporate ethanol on 80°C hot plate for 2'.
9. Deposit adhesion layer.
    - 2000Å parylene.
10. Sputter metal for ground electrodes.
    - 2500Å Au.
11. Photolithography of the 2nd mask.
    - Spin on AZ5214 photoresist at 4000rpm for 30".
    - Prebake on 75°C hot plate for 40".
    - UV exposure with mask for 60".
    - UV lamp: 350W/cm^2.
    - Develop in AZ5214 developer solution for 1'.
    - DI rinse; blow dry.
12. Etch Au ground electrodes.
    - KI:I_2:DI of 10g:2.5g:200ml for 2'.
    - DI rinse; blow dry.
13. Photoresist cleaning.
    - Strip resist with acetone.
    - O_2 plasma clean for 5' at 20W, 4mT.

14. Prepare dielectric layer.
    - Mix PDMS prepolymer and its curing agent at 4:1 volume ratio.
    - Degas the mixture at 50mT for 30'.
15. Deposit dielectric layer.
    - Spin on PDMS mixture at 3500rpm for 40".
    - Cure in 80°C oven for 4 hours.
16. Peel off from the PMMA substrate.

BIBLIOGRAPHY

[1] T. K. Jun, and C. J. Kim, "Valveless Pumping Using Traversing Vapor Bubbles in Microchannels", *Journal of Applied Physics*, Vol. 83, No. 11, pp. 5658-5664, June 1998.

[2] M. G. Lippmann, "Relations Entre Les Phénomènes Électriques Et Capillaries", *Annales De Chimie Et De Physique 5*, No. 11, pp. 494-549, 1875.

[3] J. Lee, and C. J. Kim, "Liquid Micromotor Driven by Continuous Electrowetting", *Proceedings of IEEE Micro Electro Mechanical Systems Workshop*, Heidelberg, Germany, pp. 286-291, January 1998.

[4] J. Lee, and C. J. Kim, "Microactuation by Continuous Electrowetting Phenomenon and Silicon Deep RIE Process", *Proceedings of MEMS, ASME IMECE, Anaheim*, CA., pp. 475-480, November 1998.

[5] J. Lee, and C. J. Kim, "Microactuation by Electrically-Controlled Surface Tension", *Journal of Microelectromechanical Systems*, Vol. 9, No. 2, pp.171-180, June 2000.

[6] M. A. Unger, H. P. Chou, T. Thorsen, A. Scherer, and S. R. Quake, "Monolithic Microfabricated Valves and Pumps by Multilayer Soft Lithography", *Science*, Vol. 288, pp.113-116, April 2000.

[7] B. H. Jo, L. M. Van Lerberghe, K. M. Motsegood, and D. J. Beebe, "Three-Dimensional Microchannel Fabrication in Polydiemthylsiloxane (PDMS) Elastomer", *Journal of Microelectromechanical Systems*, Vol. 9, No. 1, pp.76-81, March 2000.

[8] D. C. Duffy, J. C. McDonald, O. J. A. Schueller, and G. M. Whitesides, "Rapid prototyping of microfluidic systems in poly(dimethylsiloxane)", *Analytical Chemistry*, 70, pp.4974-4984, 1998.

[9] M. K. Chaudhury, and G. M. Whitesides, "Direct Measurement of Interfacial Interactions between Semispherical Lenses and Flat Sheets of Poly(Dimethylsiloxane) and Their Chemical Derivatives", *Langmuir*, 7, pp.1013-1025, 1991.

[10] M. K. Chaudhury, and G. M. Whitesides, "Correlation between Surface Free-Energy and Surface Constitution", *Science*, 255, pp.1230-1232, 1992.

[11] S. K. Cho, H. Moon, J. Fowler, and C-J Kim, "Splitting a liquid droplet for electrowetting-based microfluidics," *Proceedings of 2001 ASME International Mechanical Engineering Congress and Exposition*, November 11-16, 2001, New York.

[12] M. Ohring, *The Materials Science of Thin Films*, Academic Press Inc., 1992.

[13] P. J. De Pablo, J. Colchero, J. Gómez-Herrero, P. A. Serena, and A. M. Baró, "Thermal Maps of Gold Micro-Stripes Obtained Using Scanning Force Microscopy", *Nanotechnology 12*, pp.113-117, 2001.

[14] S. Zhou, P. Reynolds, R. Krause, and J. Hossack, "Finite Element Simulation of Laser Based Optical Generations of Ultrasound", *Proceedings of IEEE International Ultrasonics Symposium*, Vol. 1, pp.589-592, October 8-11, 2002, Munich.

[15] A. Subrahmanyam, V. Vasu, and P. Manivannan, "Studies on Transport Mechanism in Indium Tin Oxide (ITO) / p-Indium Phosphide (InP) Solar Cells Prepared by

Reactive Electron Beam Evaporation and Spray Pyrolysis Techniques", *IEEE Photovoltaic Energy Conversion*, Vol. 2, pp.1922-1925, 1994.

[16] E. Terzini, G. Nobile, T. Polichetti, and P. Thilakan, "Development and Application of Low Temperature Magnetron Sputtered ITO Thin Films for a-Si:H Based Junction Solar Cells", *IEEE Photovoltaic Specialists Conference*, pp.667-670, September 29 – October 3, 1997.

[17] A. H. Khalid, and A. A. Rezazadeh, "Fabrication and Characterization of Transparent-gate Field Effect Transistors Using Indium Tin Oxide", *Proceedings of IEE Optoelectronics*, Vol. 143, No. 1, pp.7-11, February, 1996.

[18] G. B. Lee, S. H. Chen, G. R. Huang, W. C. Sung, and Y. H. Lin, "Microfabricated Plastic Chips by Hot Embossing Methods and Their Applications for DNA Separation and Detection", *Sensors and Actuators B* 75, pp.142-148, 2001.

[19] K. F. Lei, W. J. Li, N. Budraa, and J. D. Mai, "Microwave Bonding of Polymer-Based Substrates for Micro/Nano Fluidic Applications", *The 12th International Conference on Solid-State Sensors, Actuators, and Microsystems (Transducers 03')* Boston, USA, June 8-11, pp.100-107, 2001.

[20] F. Niklaus, P. Enoksson, E. Kälvesten, and G. Stemme, "Low-temperature Full Wafer Adhesive Bonding", *Journal of Micromechanics and Microengineering 11*, pp.100-107, 2001.

[21] K. W. Oh, A. Han, S. Bhansali, and C. H. Ahn, "A Low-temperature Bonding Technique using Spin-on Fluorocarbon Polymers to Assemble Microsystems", *Journal of Micromechanics and Microengineering 12*, pp.187-191, 2002.

[22] S. Li, C. B. Freidhoff, R. M. Young, and R. Ghodssi, "Fabrication of Micronozzles using Low-temperature Wafer-level Bonding with SU-8", *Journal of Micromechanics and Microengineering 13*, pp.732-738, 2003.

[23] J. C. McDonald, D. C. Duffy, J. R. Anderson, D. T. Chiu, H. Wu, O. J. A. Schueller, and G. M. Whitesides, "Fabrication of Microfluidic Systems in Poly(dimethylsiloxane)", *Electrophoresis*, 21, pp.27-40, 2000.

[24] K. F. Lei, R. H. W. Lam, J. H. M. Lam, and W. J. Li, "Polymer Based Vortex Micropump Fabricated by Micro Molding Replication Technique", submitted to *2004 IEEE/RSJ International Conference on Intelligent Robots and Systems*.

[25] J. Kim, W. Shen, L. Latorre, and C. J. Kim, "A Micromechanical Switch With Electrostatically Driven Liquid-Metal Droplet", *Sensors and Actuators A*, 97-98, pp. 672-679, 2002.

[26] S. K. Fan, P. P. De Guzman, and C. J. Kim, "EWOD Driving Of Droplet On N×M Grid Using Single-Layer Electrode Patterns", *Technical Digest, Solid-State Sensor, Actuator, and Microsystems Workshop*, Hilton Head Island, SC, pp. 134-137, June 2002.

[27] S. K. Cho, S. K. Fan, H. Moon, and C. J. Kim, "Towards Digital Microfluidic Circuits: Creating, Transporting, Cutting and Merging Liquid Droplets By Electrowetting-Based Actuation", *IEEE Conference of Micro Electro Mechanical Systems*, Las Vegas, NV, pp.97-100, January 2002.

[28] Product Sheet of Sylgard® 184 Silicone Elastomer, Dow Corning.

[29] Product Sheet of Teflon® AF Amorphous Fluoropolymers, Dupont.

[30] Product Sheet of Parylene C, Specialty Coating Systems, Cookson Electronics.

[31] H. Moon, S. K. Cho, R. L. Garrell, and C. J. Kim, "Low Voltage Electrowetting-On-Dielectric", *Journal of Applied Physics*, Vol. 92, No. 7, pp. 4080-4087, October 2002.

[32] J. Lee, H. Moon, J. Fowler, T. Schoellhammer, and C. J. Kim, "Electrowetting and Electrowetting-on-dielectric for Microscale Liquid Handling", *Sensors and Actuators A*, 95, pp.259-268, 2002.

[33] H. J. J. Verheijen, and M. W. J. Prins, "Reversible Electrowetting and Trapping of Charge: Model and Experiments", *Langmuir*, 15, pp.6616-6620, 1999.